NASA Contractor Report 172465

DEVELOPMENT OF FAILURE CRITERION FOR KEVLAR/EPOXY FABRIC LAMINATES

NASA-CR-172465
19850002830

R. C. TENNYSON AND W. G. ELLIOTT

UNIVERSITY OF TORONTO
Institute for Aerospace Studies
Toronto, Ontario, Canada

NASA
National Aeronautics and
Space Administration

Langley Research Center
Hampton, Virginia 23665

TABLE OF CONTENTS

1.0 INTRODUCTION

In the construction of laminated composite structures, the fabricator can select from a wide range of composite material systems. Generic materials such as glass, graphite and aramid fibers (such as Kevlar™) are available both in the "dry" and "prepreg" forms, to satisfy a diverse set of design requirements. Depending on the application, one can fabricate components by filament or tape winding methods, or by laying up a configuration utilizing commercial prepreg materials which meet relatively stringent quality control criteria (in terms of resin/fiber content, volatile content as well as specified physical/mechanical properties). In the case of prepreg systems, the manufacturer has the option of choosing between unidirectional and woven fabric formats. However, when one considers manufacturing and design requirements, it is often more cost-effective to utilize the woven fabric system.

One major problem area that continues to plague the design engineer is the selection of suitable strength criteria for composite laminates, regardless of the material system and manufacturing process being used. In aerospace construction, one usually encounters relatively thin-walled structures and thus, to a first approximation, a plane stress state can be assumed to exist for preliminary design purposes. However, it is becoming increasingly evident that in many instances, three-dimensional stress effects must be considered, particularly in the vicinity of free edges (associated with joints, cutouts, fasteners, etc.). Indeed, such effects can lead to delamination and/or crack initiation which are of major concern to the analyst. Regardless of the stress state, the requirements for lamina and overall structural failure criteria still persist. The most desirable failure model is one which can provide conservative maximum load estimates of reliable accuracy. However, the model must not be so conservative that

2

it jeopardizes the design itself in terms of increasing the weight needlessly. On the other hand, it should be relatively operationally easy to employ, and not be dependent on the development of such an extensive data base using complex and expensive test procedures that the user shuns its application. One might comment that the presence of local stress concentrations (due to cracks, free edges, holes, etc.) does not influence the form of a <u>lamina</u> strength criterion. Rather, such considerations can be taken into account in the formulation of the stress analysis and the failure criterion one adopts for the whole laminate. For example, if one is performing a finite element analysis, including three-dimensional stress terms, failure is determined not only by the <u>lamina failure model</u>, but equally as important, by the <u>laminate failure model</u> one assumes.

Lamina failure models can essentially be grouped into three categories of increasing operational complexity. The simplest approach is to design to maximum stress or strain (which are not equivalent criteria). Unfortunately, these models lead to substantial "over-estimates" of strength in the "corner" regions of the failure surface envelope. The next class of models are those which approximate the failure surface by quadratic polynomials of different forms. Many variations of quadratic models can be found in the literature, including ones which define the surface using different functions for each quadrant. Again, it has been demonstrated that, for certain load cases, quadratic formulations can overestimate strength as well (Ref. 1). In some instances, such as biaxial loading, the quadratic criterion can under predict strength by as much as 30%-40% (Ref. 2). The third category of failure criteria is termed "higher order models", the most common one of which is the "cubic" polynomial (Refs. 1, 2, 3). It should be noted that all of the above mentioned formulations represent approximations encompassed by the general "tensor polynomial"

criterion advocated in Ref. 3. The one feature that is common to all of these lamina failure models is that they represent a phenomenological, macro-mechanics approach to predicting lamina failure. They all attempt to describe the real failure surface in stress (or strain) space. Table 1 presents a summary of the test data and interaction strength parameters that one would require for each classification of failure model. It becomes quite apparent that the higher order cubic model demands more baseline strength data. This of course raises the question as to whether or not the additional complexity (and cost) is warranted. As noted earlier however, there do exist regions of the failure surface (for a plane stress state) where indeed such a criterion is required. This has been well documented elsewhere (see Refs. 1,2).

The issues addressed in this report concern an investigation of woven fabric laminates and can be summarized as follows:

- develop a failure model that best characterizes laminates constructed from woven fabric prepreg materials;

- render the cubic polynomial failure criterion operationally easier to apply;

- develop a laminate stress analysis model for woven fabric laminates.

The major objective of this work is to develop a data base derived from woven fabric laminate tests from which a failure criterion can be formulated. Since it is known that the cubic polynomial models works well for laminates constructed from undirectional materials, this criterion will serve as a reference basis. At the same time, however, it will be demonstrated how this higher order model can be cast into a set of design curves suitable for use in preliminary strength estimates, without recourse to the additional tests described in Table 1 or the solution of a cubic

equation. This interim report summarizes the results obtained to-date based on one woven fabric prepreg system:

Narmco 5208 - K285 (Kevlar™ 49, 4 harness satin) with 50% resin and 2% volatile content (by weight), requiring a 350°F cure temperature at 90 psi pressure.

2.0 MATERIAL DESCRIPTION

The woven fabric prepreg used in this first phase of the program was Narmco 5208 - K285 - a four harness (over 3, under 1) weave of Kevlar™ 49 filaments impregnated with Narmco 5208 epoxy resin. Two major concerns that arise when one examines a woven fabric prepreg are the relative angles between the warp and fill and the degree of fiber straightness. The 0°, or warp direction, fibers are very straight and parallel. However, the 90°, or fill direction fibers, while parallel to each other, are not straight or orthogonal to the 0° fibers. The angle between the warp and fill direction fibers was found to vary by up to 15°. The effect that this fiber misalignment has on the strength and stiffness of the material will be discussed later.

3.0 MANUFACTURING AND TEST PROCEDURES

3.1 Manufacture of Specimens

Both tubular and flat samples were manufactured using the Narmco standard autoclave cure cycle. One ply of resin bleeder per ply of prepreg was used, which yielded a cured thickness of 0.007" per ply. Cure temperature used was 350°F with 90 psi pressure, although the optional post-cure was not performed since all testing was conducted at room temperature.

After fabrication, the specimens were cut to the proper size by using a high speed abrasive disk. The apparatus employed for cutting the flat specimens is shown in Figure 1. Tubular specimens were cut by mounting them on a lathe and using an air powered cutting disk as shown in Figure 2.

One of the problems encountered during the testing program resulted from the fill direction fiber misalignment, as noted earlier. Thus it was decided to try and straighten the fibers prior to the specimen layup. This was accomplished by clamping one edge of the material and then pulling the material until the fill direction fibers were straight. Care must be taken to ensure that the warp direction fibers remain straight during this process. This procedure was successful in providing specimens with fibers straight in both directions and nearly orthogonal to each other. However, it was found to work well only for small sections of material and is not suggested for large scale work. It must be emphasized that pre-straightening and alignment is necessary to obtain optimum properties of the material in it's correct orientation. Only in this way can one achieve maximum strength (and stiffness) for various load conditions and ply orientations.

3.2 Tension Tests

The specimens used in the tension tests were 3 ply, 2" wide by 6" long, flat coupons. Aluminum end tabs 2" wide × 1 1/2" long × 1/8" thick were attached to both ends using American Cynamid FM300 adhesive film. The end tabs were held in place while curing, with the potting grip fixture shown in Figure 3. The film adhesive was cured at 350°F for one hour.

Strain gauges were then applied to the specimen to measure both the axial and transverse strains. Gauges were used on both sides of the specimen to measure the amount of bending that was present during testing.

Each specimen was placed in a set of end grips which were mounted in a Tinius Olsen, 4 screw, electrically driven test machine. A set of gimballed end fittings were also used to minimize any bending moments from being applied to the specimen. The specimen grips are shown in the testing machine in Figure 4.

Load and strain readings were taken using an Optilog data acquisition system and stored in an Apple II plus microcomputer. These results were then employed to calculate the tensile module E_{11_T} for the 0° samples, E_{22_T} for the 90° samples and the Poisson ratio's V_{12} and V_{21}. These tests also provided the 0° strength (X), 90° strength (Y) and ultimate strains, $\varepsilon_{1_{ult_T}}$ and $\varepsilon_{2_{ult_T}}$.

3.3 Compression Tests

The specimens used for compression testing were 20 plies thick, 0.75" wide by 3.5" long. Aluminum end tables .75" wide by 1.5" long by 1/16" thick were bonded on with Hysol 9340 adhesive, a room temperature curing epoxy.

The specimens were then mounted in an IITRI-type compression fixture as shown in Figure 5. The test fixture was subsequently placed in the Tinius Olsen testing machine and the load applied through a hardened steel loading bar.

Strain gauges were mounted on both sides of the specimen to measure axial strains. Due to the specimen size, transverse strain measurements were not taken. It is very important to have gauges on both sides of the specimen since they can be used to determine whether failure occurs due to buckling, and to calculate the amount of bending stress applied to the coupon. These considerations are very important in compression testing, while not as significant in tension tests.

7

As with the tension tests, the load and strain data were collected using the Optilog and Apple II microcomputer. From this data, the compressive moduli E_{11C} and E_{22C} were calculated as well as the strengths X'(0°), Y'(90°) and the maximum strains, ε_{1ult_C} and ε_{2ult_C}.

3.4 Torsion Tests

The torsion tests were performed using tubular specimens, 2" in diameter, 6" long and varying from 3 to 8 plies thick. The tubes were bonded into circular aluminum end pots using Hysol 6175 resin and 3561 hardener. They were centrally mounted and aligned orthogonal to the base of both end pots. The tubes were positioned in a torsion fixture attached to the Tinius Olsen, which served as a rigid base. Torque loading was applied by two hydraulic pistons which were connected to a circular plate, fastened to the top of the tube. The pistons were then pressurized by a hand operated pump. A view of the test setup is shown in Figure 6.

A pressure transducer was connected to the hydraulic pistons, thus providing the data necessary to calculate the applied torque. Strain gauges were bonded on the specimen at ± 45° to the tube's longitudinal axis. These gauges provided the shear strain present in the sample. The pressure and strain data were collected using the same data acquisition system described earlier and used to calculate the material shear modulus G_{12}. The other data resulting from these tests are the shear strength (S) and the maximum shear strain (γ_{ult}).

3.5 Biaxial Load Tests

In order to calculate the interaction parameters for the failure theory, it was necessary to perform some biaxial loading tests. For woven fabric materials, internal pressure tests on 0° or 90° tubes will provide

the proper stress state. If one considers the cubic form of the failure equation, then three points are required for solving F_{12}, F_{112} and F_{122}. Three test configurations were selected; 0° and 90° internal pressure, and 0° internal pressure with axial compression.

The specimens fabricated for these tests were 3 ply, 4" diameter by 6" long tubes. The larger diameter tubes were used to reduce the amount of wall wrinkling during curing. It was necessary to eliminate the wrinkles since they caused premature failure where the fibers were bent. The tubes were made with a continuous wrap of prepreg to obtain all three plies. This was done because failure occurs predominantly from the failure of the hoop direction fibers. It was also necessary to reinforce the area where the fibers ended, to prevent premature failure from occurring there.

The tubes, once manufactured, were again potted into aluminum end fittings using Hysol 6175 and 3561. The end fittings were connected to an air operated hydraulic pump and the tube filled with oil. In this procedure, the pump was used only to pressurize a reservoir. Subsequently, by opening a valve between the reservoir and the tube, the pressure in the tube was increased slowly until failure occurred. The pressure test setup is shown in Figures 7 and 8. Axial and circumferential gauges were employed to verify the tube stiffness and to record the strains at failure. In addition, a pressure transducer was placed at the inlet to the specimen, thus permitting the pressure and strain values to be recorded as before. At the same time, they were monitored on an x-y plotter to provide control of the loading rate.

For the combined compression-pressure test, the same procedure as above was used, only the tube was placed in the Tinius Olsen below a loading platen. The specimen was then subjected to a specific ratio of pressure to compressive loading so that the net axial stress applied to the tube was

9

compressive. This process was also controlled by monitoring the pressure transducer and the load, all on an x-y plotter, and then following a preset loading curve. Strain values were recorded in the same manner as the pressure tests.

The results from these tests yielded ultimate failure pressures which defined the stress state at failure σ_{1ult}, σ_{2ult} and the strain state at failure ε_{1ult}, ε_{2ult}.

To determine the shear interaction terms F_{166} and F_{266}, a combined tension-torsion test was performed. The method of torsion loading was identical to that described previously, with the addition of a tensile load applied simultaneously. As with the pressure-compression test, the loading followed a prescribed ratio of tensile load to torque. The test facility is shown in Figure 9. Both 0° and 90° tubes were investigated to calculate the two interaction terms. The specimens used were 2" diameter tubes, 5" long and were mounted in the same manner as the torsion test samples.

4.0 DISCUSSION OF TEST RESULTS

4.1 Tension

The results of the tension tests are presented in Table 2 for the 0° specimens and Table 3 for the 90° specimens. Sample stress-strain curves are also shown in Figures 10 and 11 for the 0° and 90° tests, respectively.

Examining first the 0° test results, the average ultimate strength X is 86.1 ksi, the modulus of elasticity E_{11T} is 5.72×10^6 psi, the Poisson ratio V_{12} is 0.072 and the strain to failure ε_{ult_T} is 1.50%. The results are very repeatable, with the variance in strength, modulus and ultimate

10

strain all being less than 6% of their average values. However, the Poisson ratio varies more than the other values, due to the small magnitude of the strains being measured.

As can be seen in Figures 10 and 11, this material is linear to failure in tension. The amount of bending in the sample, as shown by the difference in the two curves, is very small, so corrections to the ultimate stress due to bending stresses are not required.

The results of the 90° tension tests are more difficult to explain. From Table 3a, it can be seen that there is a large variance in both the strength and modulus results, with strength varying from 25 ksi to 65 ksi and modulus varing from (2.6 to 6.) $\times 10^6$ psi. After further examination of the specimens, the misalignment angle relative to the 90° fibers was measured and the strength and modulus plotted as a function of this angle. Figure 12 shows the ultimate strength vs. angle and Figure 13 shows E_{22_T} vs. angle. As can be seen in both Figures 12 and 13, the misalignment angle greatly affects the strength and modulus of the material. The theoretical curves shown were calculated using two different models. The off-axis laminate analysis retained orthogonality of fibers but simply rotated the laminae by the amount of the misalignment angle. The second form of analysis considered rotation of only the 90° fibers while maintaining a constant alignment of the 0° fibers. In this case, the ratio of fiber to matrix modulus of the material must be known, as described in the Appendix. Various ratios were assumed and the resulting curves derived.

Due to the large effect that the fiber misalignment has on the modulus and strength, it was decided to manufacture more specimens, incorporating pre-straightening of the fibers prior to curing. The results of these tests are presented in Table 3b. One can immediately see that the strength obtained in these tests is significantly higher than the previous 90° data,

11

while the modulus varies only slightly. This is probably due to premature failure in the first test series from the 90° fibers being curved, even though the average direction is nominally perpendicular to the 0° fibers. The average values taken for the 90° direction are for the strength Y = 80.2 ksi, the modulus E_{22T} = 5.76 × 10^6 psi, and Poisson's ratio, V_{21} = 0.071.

Ideally the strength and modulus in the two directions should be the same. In fact, only the modulus and Poisson ratios are very close for the two directions and thus average values of E_T = 5.74 × 10^6 psi and V = 0.072 will be used in further calculations. However, the strengths differ due to the way in which the material is woven, and consequently they will be used separately in calculating the failure solutions.

4.2 Compression

The compression test results are presented in Tables 4 and 5 for the 0° and 90° tests, respectively. Stress-strain curves are also given for the 0° and 90° samples in Figures 14 and 15, respectively.

For the 0° samples, the average results give an ultimate strength X' = 26.9 ksi and an initial linear modulus E_{11C} = 4.12 × 10^6 psi with an ultimate strain, ε_{1ult_C} = 2.86%. The variance in the ultimate stress is about 3% of the average value, while the modulus varies by up to 9%.

From Figure 14, it can be seen that the stress-strain curve is not linear to failure, and in fact appears to be bilinear. The average modulus of the second section is 0.45 × 10^6 psi, with the point of inflection occuring at an average stress of 14.8 ksi, which is 55% of the ultimate compressive stress.

The 90° compression results are very similar to those found in the 0° tests. The ultimate stress Y' = 26.5 ksi, the initial modulus E_{22C} = 4.50 × 10^6 psi, and the ultimate strain ε_{2ult_C} = 2.91%. The ultimate stresses and

12

moduli vary by 4% and 6%, respectively.

As seen in Figure 15, the stress-strain curve is also bilinear in the 90° direction, similar to the 0° compression tests. The "knee" stress occurrs at 15.0 ksi (57% of ultimate) and the modulus of the final section is 0.45×10^6 psi.

Since the 0° and 90° strength and modulus are nearly the same, an average value can be used: $E_{11C} = E_{22C} = 4.31 \times 10^6$ psi, $X' = Y' = 26.7$ ksi, $\sigma_{knee} = 14.9$ ksi and $E_{final_C} = 0.45 \times 10^6$ psi.

Due to the nonlinearity of the material in compression, no correction in the compressive strength due to bending was made. Compressive failure was ensured by making the samples sufficiently thick to prevent buckling prior to failure.

4.3 Torsion

The results of the torsion tests for determining the shear properties of the material are given in Tables 6 and 7 for the 0° and 90° tubes, and Figures 16 and 17 present typical stress-strain plots.

Since the shear properties of the material should be the same in the 0° and 90° directions, one should examine both Tables 6 and 7 together. It can be seen that the shear strength increases with increasing number of plies. This is due to the thin specimens failing initially from torsional buckling. The 8 ply 90° samples did not buckle at failure and thus their strength is representative of the material shear strength. It can be seen that the shear moduli for both types of specimens fall into the same range so an average value will be used. The ultimate shear strains differ approximately in proportion to the ratio of ultimate stresses. Hence the 90° ultimate strain is taken as the strain to failure. In summary, the shear properties are given by: the shear strength S = 13.51 ksi, the shear modulus G_{12} =

0.380×10^6 psi, and the ultimate shear strain $\gamma_{ult} = 5.38\%$.

The shear stress-strain curves shown in Figures 16 and 17 demonstrate that this material is non-linear in shear. The shear modulus calculated is based on the initial linear section which approximates the response up to about 50% of the ultimate stress. The larger variance in shear modulus from one test to another was partially a result of the differing degrees of non-linearity observed between tests.

5.0 BIAXIAL LOAD TESTS

5.1 Internal Pressure Tests

In order to determine the interaction strength parameters, it was necessary to perform a series of biaxial load tests. The simplest of these is an internal pressure test. This test gives a stress ratio σ_x/σ_y of 1/2. For the weave material, since the strength in both directions is approximately equal, then one can employ either a 0° or 90° tube. The results of these tests are presented in Tables 8 and 9 for both 0° and 90° tubes, respectively.

Because the Kevlar™ fibers are quite flexible, great care was needed to prevent the fibers from wrinkling while curing. Of the results given in Tables 8 and 9, only half of them are acceptable since failure occurred in an area weakened by wrinkling in the other tests.

Figures 18 and 19 provide typical pressure-strain curves for the 0° and 90° tests, respectively. As expected, the material is linear to failure under these conditions. Furthermore, the biaxial tension testing gives strength values which exceed the unidirectional tension strengths.

14

5.2 Pressure-Compression Test

The purpose of this test was to obtain a failure with σ_2 positive and σ_1 negative, in order to complete the testing necessary to define F_{12}, F_{112} and F_{122}. The result of this test is given in Table 10 where the resultant principal stresses at failure are σ_1 = -28.5 ksi and σ_2 = 57.2 ksi. As predicted by the theory, the internal pressure prevents failure from occurring until the axial stress is greater than the compressive ultimate stress. This particular test result together with those obtained for pressure loading are plotted in the $\sigma_1 - \sigma_2$ plane as shown in Fig. 20. The analytical models also presented in Fig. 20 will be discussed later.

5.3 Tension - Torsion Tests

One can again refer to Table 10 for a summary of these test results. Considerable difficulty in achieving "good" failures was experienced due to torsional buckling, and specimen failure in an area where the fibers wrinkled during the curing stage. Although the data presented represent the "best" of the tests performed, there was still some minor fiber wrinkling in the tubes. Consequently, these specimens may have failed somewhat prematurely. However, it is felt that since failure was not localized about the "wrinkled" region, the loads are reasonably accurate.

The test results are plotted in Figs. 21 and 22 for the $\sigma_1 - \sigma_6$ and $\sigma_2 - \sigma_6$ planes, respectively. Based on these data, one can then calculate the two interaction parameters F_{166} and F_{266}.

6.0 FAILURE MODEL FOR WOVEN FABRIC LAMINATES

Although it is premature to generalize at this time, based on the test results for the particular Narmco 5208 - K285 Kevlar™ prepreg investigated, some interesting observations can be made.

First, the reader is referred to Table 11 which summarizes the data and properties measured to-date. From these results, one can readily calculate the strength parameters associated with the quadratic and cubic tensor polynomial failure criteria. For reference purposes, the general form of this criterion is (Ref. 3),

$$F_i\sigma_i + F_{ij}\sigma_i\sigma_j + F_{ijk}\sigma_i\sigma_j\sigma_k + \ldots = f(\sigma) = \begin{cases} < 1 \text{ no failure} \\ 1 \text{ failure} \\ > 1 \text{ exceeded failure} \end{cases} \qquad (1)$$

for $i, j, k = 1\ldots6$. F_i, F_{ij} and F_{ijk} are strength tensors of the 2nd, 4th and 6th rank, respectively. For the case of a plane stress state, Eq. (1) reduces to (see Refs. 1, 2, 3),

$$F_1\sigma_1 + F_2\sigma_2 + F_{11}\sigma_1^2 + F_{22}\sigma_2^2 + F_{66}\sigma_6^2 + 2 F_{12}\sigma_1\sigma_2 + 3 F_{112}\sigma_1^2\sigma_2 +$$

$$3 F_{122}\sigma_1\sigma_2^2 + 3 F_{166}\sigma_1\sigma_6^2 + 3 F_{266}\sigma_2\sigma_6^2 = 1 \qquad (2)$$

if one retains cubic terms. The principal strength parameters are defined by,

$$F_1 = \frac{1}{X} \frac{1}{X'}, \qquad F_2 = \frac{1}{Y} \frac{1}{Y'}, \qquad F_{11} = \frac{1}{XX'}, \qquad F_{22} = \frac{1}{YY'}, \qquad F_{66} = \frac{1}{S^2} \qquad (3)$$

where X, Y define tensile strengths in the fiber (or warp) and matrix (or fill) directions, respectively; X', Y' define the corresponding compressive strengths and S is the shear strength measured in the principal material

axes plane. The interaction terms include F_{12}, F_{112}, F_{122}, F_{166} and F_{266}. The corresponding quadratic form of Eq. (2) is,

$$F_1\sigma_1 + F_2\sigma_2 + 2 F_{12}\sigma_1\sigma_2 + F_{11}\sigma_1^2 + F_{22}\sigma_2^2 + F_{66}\sigma_6^2 = 1 \qquad (4)$$

In many cases, F_{12} is taken equal to zero, although many authors select $F_{12} = -\frac{1}{2}(F_{11}F_{22})^{1/2}$ to ensure a "closed" failure surface in stress space. The consequences of this assumption will be made clear later as it relates to the analysis of fabric laminates.

Based on Eq. (3), one can calculate the principal strength parameters from the data listed in Table 11. Furthermore, using the biaxial failure data presented in Tables 8, 9, 10 and using Eq. (2), one can then solve for the interaction parameters noted above. Table 12 provides a summary of the full set of strength parameters required for a cubic model representation of the failure surface. Plots of the three planes $\sigma_1 - \sigma_2$, $\sigma_1 - \sigma_6$ and $\sigma_2 - \sigma_6$ have been mentioned earlier, and one can again refer to Figs. 20-22 to see the cubic solutions. However, of more interest is the fact that if one employs only the quadratic model [Eq. (4)] with $F_{12} = 0$, equally as good a fit to the test data occurs. In other words, a cubic model, and all the complexity and additional tests required to evaluate the interaction terms, is not necessary to predict strength for fabric laminates. The same degree of accuracy can be obtained using the quadratic model with $F_{12} = 0$. This latter point should be emphasized because if one plots the quadratic solution assuming $F_{12} = -\frac{1}{2}(F_{11}F_{22})^{1/2}$, one obtains a failure curve in the $\sigma_1 - \sigma_2$ plane that grossly overestimates strength, as evident in Fig. 20.

A note of caution should be issued at this point because it is not known to what extent the orthotropic fabric strengths must differ before one

17

is faced with the requirement of using a higher order failure model. One does know that, for example, laminae formed from unidirectional prepregs, where the tensile strength ratios $(\frac{X}{Y})$ are of the order of 20, the cubic model works best. Clearly a transition must take place as $X/Y \rightarrow 1.0$.

7.0 <u>REDUCTION OF CUBIC MODEL FOR DESIGN PURPOSES</u>

One of the major problems in the utilization of a higher order failure criterion such as the cubic model, is the difficulty involved in evaluating the additional strength parameters (see Ref. 2 for example). For the design engineer and analyst, if the data are not available, one simply cannot apply the criterion and recourse to simpler models is necessary. In this section, an attempt has been made to reduce the known cubic model strength data to an "operationally easier" form. As a reference basis it will be assumed that the minimum strength data available to the engineer include unidirectional measurements of the fiber and matrix dominated tensile and compressive strengths (i.e.: X, X', Y, Y') together with the shear strength (S) in the principal material axes plane. Thus, for a plane stress state, one can employ the quadratic model [Eq. (4)] with $F_{12} = 0$.

If one now considers the difference in solutions between the cubic and quadratic models for given values of the load vector (defined by the co-ordinates R, Θ, $\emptyset$ in $\sigma_1 - \sigma_2 - \sigma_6$ stress space - see Fig. 23), "design factors" can then be calculated for "correcting" the quadratic strength predictions. The curves shown in Fig. 24 were generated for the unidirectional 3M, graphite/epoxy prepreg SP288-T300 material reported in Ref. 2. An expanded view of the range $0 < \Theta < 40°$ is shown in Fig. 25. The application of these curves requires knowledge of the ply stresses

throughout the laminate. One can then calculate R, Θ, $\emptyset$ as given by

$$R = (\sigma_1{}^2 + \sigma_2{}^2 + \sigma_6{}^2)^{1/2}$$

$$\Theta = \tan^{-1} (\sigma_2/\sigma_1) \tag{5}$$

$$\emptyset = \tan^{-1} (\sigma_6/R)$$

for each ply. Note that the restricted range of $\emptyset$ angles shown is due to the very small strength values associated with σ_2 and σ_6 (i.e.: Y, Y' and S) relative to the fiber strengths (X, X'). For such unidirectional prepregs, the failure surface is highly elongated along the σ_1 axis which is typical of the materials investigated to-date. These curves can be regarded as providing non-dimensional "correction factors" and thus one does not need to evaluate the interaction terms. Again, a note of caution is in order since only graphite/epoxy and glass/epoxy have been investigated and clearly more data on other unidirectional prepregs would be valuable before generalizations about the application of these curves can be made.

The main advantage of this form of solution presentation is that the design engineer can determine if indeed his stress state puts him into a conservative zone (+'ve ordinate) or in a region where the cubic model indicates that the quadratic solution "overestimates" the lamina strength (-'ve ordinate). In this latter case, appropriate safety factors could then be applied to the stress analysis.

As a final comparison, the previous results for the Narmco 5208-K285 woven fabric prepreg have been presented in this form in Fig. 26. One can readily see, as expected, that the correction factors needed for the quadratic model are quite small and in fact are insignificant.

8.0 CONCLUDING REMARKS

(a) The quadratic failure criterion with $F_{12} = 0$ provides accurate estimates of failure stresses for the woven fabric prepreg investigated in this report. It is anticiated that present work on a graphite/epoxy woven fabric prepreg will also yield a similar conclusion.

(b) The cubic failure criterion has been re-cast into an operationally easier form, providing the engineer with design curves that can be applied to laminates fabricated from unidirectional prepregs. In the form presented, no interaction strength tests are required, although recourse to the quadratic model and the principal strength parameters is necessary. However, insufficient test data exists at present to generalize this approach for all unidirectional prepregs and its use must be restricted to the generic materials investigated to-date.

REFERENCES

1. Tennyson, R.C., Nanyaro, A.P. and Wharram, G.E., "Application of the Cubic Polynomial Strength Criterion to the Failure Analysis of Composite Materials", J. Composite Materials Supplement, Vol. 14, 1980.

2. Tennyson, R.C. and Elliott, W.G., "Failure Analysis of Composite Laminates Including Biaxial Compression", NASA CR 172192, August 1983.

3. Tsai, S.W. and Wu, E.M., "A General Theory of Strength for Anisotropic Materials", J. Composite Materials, Vol. 5, 1971.

Table 1   Plane Stress Failure Model Test Requirements*

Failure Model	Test Requirements
Max. Stress or Strain (1)	0° tension, compression 90° tension, compression 0° or 90° shear
Quadratic (2)	Same as (1), with option to evaluate interaction term F_{12} analytically (using "closure" condition) or with biaxial tension test

Cubic (3)	Same as (1) with requirement to evaluate: F_{12}, F_{112}, F_{122}, F_{166}, F_{266}
	
	Minimum requirements: Biaxial tenstion test
	                            + 4 constraint eq.
	Preferable: Biaxial tension, biaxial compression
	                     + 2 constraint eq. (see Refs.1,2)

*   These hold for an orthotropic material, such as unidirectional
    prepreg or woven (orthotropic) fabric. In the latter case 0°
    and 90° refer to warp and fill directions, respectively.

Table 2   0° (Warp Direction) Tension Test Results

Test #	σ_{1ult}(ksi)	$E_{11T}(10^6$ psi)	V_{12}	ε_{1ult_T}(%)
1	87.8	5.92	0.085	1.44
2	89.3	5.69	-----	1.55
3	85.6	5.98	0.065	1.41
4	85.5	5.76	0.079	1.55
5	82.5	5.38	0.059	1.55
AVG:	86.1	5.72	0.072	1.50

Table 3   90° (Fill Direction) Tension Test Results

Table 3a   Unstraightened

Test #	Angular Deviation From 90°	σ_{2ult}(ksi)	$E_{22T}(10^6$ psi)	V_{21}	ε_{2ult_T}(%)
1	1	55.8	6.05	0.072	0.92
2	12	27.3*	2.69*	0.079	1.20
3	13	24.0*	2.61*	0.069	1.01
4	1	56.6	5.68	0.025	1.00
5	9	43.7*	3.59*	-----	1.43
6	15	24.9*	2.60*	0.082	1.39
7	5	52.2*	4.32*	0.055	1.17
8	8	42.8*	3.98*	-----	1.17
9	7	47.2*	4.20*	-----	1.41
10	0	65.4	5.60	-----	1.18
AVG:		59.3	5.78	0.071	1.19

Table 3b   Straightened Material

Test #	σ_{2ult}(ksi)	$E_{22T}(10^6$ psi)	ε_{2ult_T}(%)
11	82.6	5.94	1.37
12	64.9*	5.57	1.13*
13	79.8	----	----
14	78.3	----	----
AVG:	80.2	5.76	1.37

* Not included in calculating average value

Table 4   0° (Warp Direction) Compression Test Results

Test #	# of Plies	σ_{1ult} (ksi)	E_{11C} (10^6 psi)	ε_{1ult_C} (%)	σ_{knee} (ksi)	E_{11C}fin (10^6 psi)
1	12	21.9*	4.15	2.32*	13.7	----
2	12	23.4*	4.38	----	14.6	0.44
3	12	21.6*	4.12	----	14.5	----
4	20	27.5	3.88	2.30	14.1	0.51
5	20	26.3	4.12	3.13	15.3	0.37
6	20	26.5	----	----	----	----
7	20	27.3	3.83	3.12	14.2	0.47
8	20	26.7	4.01	3.01	16.0	0.44
9	20	27.8	4.09	----	15.8	0.46
10	20	26.3	4.48	2.73	14.8	0.47
AVG:		26.9	4.12	2.86	14.8	0.45

NOTE: * Not included in calculating average value.

Table 5   90° (Fill Direction) Compression Test Results

Test #	# of Plies	σ_{1ult} (ksi)	E_{11C} (10^6 psi)	ε_{1ult_C} (%)	σ_{knee} (ksi)	E_{11C}fin (10^6 psi)
1	20	26.8	4.50	2.96	16.0	0.47
2	20	26.6	4.75	2.72	14.8	0.46
3	20	26.5	4.33	3.04	14.6	0.45
4	20	27.1	4.31	3.24	14.9	0.38
5	20	25.4	4.59	2.58	14.5	0.49
AVG:		26.5	4.50	2.91	15.0	0.45

25

Table 6   0° (Warp Direction) Torsion Test Results

Test #	# of Plies	τ_{ult}** (ksi)	G_{12} (10^6 psi)	γ_{ult} (%)
1	3	4.59*	0.377	1.46*
2	3	6.65*	0.397	1.94*
3	6	10.09	0.394	4.03
4	6	8.61	0.449	2.52
5	6	9.69	0.392	4.07
6	6	9.15	0.385	3.45
7	6	8.65	0.363	5.00
8	6	----	0.386	----
AVG:		9.24	0.393	3.82

NOTE: * Not used in calculating averages

** These "ultimate" stresses correspond to initial torsional
   buckling followed by material failure.

Table 7   90° (Fill Direction) Torsion Test Results

Test #	# of Plies	τ_{ult} (ksi)	G_{12} (10^6 psi)	γ_{ult} (%)
1	8	11.98	0.428	3.99
2	8	12.93	0.362	5.70
3	8	-----	0.320	-----
4	8	11.63	0.313	4.61
5	8	14.84	0.354	6.28
6	8	16.20	0.393	6.33
AVG:		13.51	0.362	5.38

Table 8   0° (Warp Direction) Internal Pressure Test Results

Test #	σ_{1ult} (ksi)	σ_{2ult} (ksi)	ε_{1ult} (%)	ε_{2ult} (%)
1	40.9*	81.8*	0.57	1.55
2	45.2	90.4	0.57	1.84
3	39.5*	78.9*	0.58	1.61
4	44.0	88.0	0.61	1.75
AVG:	44.6	89.2	0.58	1.69

NOTE: * Not used in calculating average value due to
            fiber wrinkling.

Table 9   90° (Fill Direction) Internal Pressure Test Results

Test #	σ_{1ult} (ksi)	σ_{2ult} (ksi)	ε_{1ult} (%)	ε_{2ult} (%)
1	85.0*	42.5*	-----	-----
2	95.8	47.9	1.84	0.69
3	88.9*	44.5*	----	----
4	96.0	48.0	1.83	0.69
AVG:	95.9	48.0	1.84	0.69

NOTE: * Not used in calculating average value due to
            fiber wrinkling.

Table 10   <u>Interaction Strength Tests</u>

Test #	Load Conf.	Angle Deg.	No. Plies	σ_{1ult} (ksi)	σ_{2ult} (ksi)	τ_{ult} (ksi)	ε_{1ult} (%)	ε_{2ult} (%)	γ_{ult} (%)
1	Pressure-Compression	0	3	-28.5	57.2	0.0	-0.47	-----	0.0
2	Tension-Torsion	0	5	28.4	0.0	15.4	0.45	0.0	1.87
3	Tension-Torsion	90	7	0.0	30.5	15.5	-----	-----	----
4	Tension-Torsion	90	7	0.0	33.5	14.7	-----	-----	----

Table 11   <u>Material Properties Summary</u>

Property	0° (Warp)	90° (Fill)	Average Value*
$E_{Tension}(10^6 psi)$	5.72	5.76	5.74
Poisson ratio	0.072	0.071	0.072
$\varepsilon_{ult_T}(\%)$	1.50	1.37	1.48
$\sigma_{ult_T}(ksi)$	86.1	80.2	83.2
$E_{compression}(10^6 psi)$	4.12	4.50	4.31
$E_{final\ comp.}(10^6 psi)$	0.45	0.45	0.45
$\varepsilon_{ult_C}(\%)$	2.86	2.91	2.89
$\sigma_{ult_C}(ksi)$	26.9	26.5	26.7
$\sigma_{knee_C}(ksi)$	14.8	15.0	14.9
$G_{12}(10^6 psi)$	0.393	0.362	0.380
$\tau_{ult}(ksi)$	-----	13.51	13.51
$\gamma_{ult}(\%)$	-----	5.38	5.38

*   Weighted according to number of samples tested in each category

Table 12   Summary of Strength Parameters

Principal Strength Parameters Eq. (3)	F_1 -2.552×10^{-5} PSI^{-1}	F_2 -2.531×10^{-5} PSI^{-1}	F_6 0
	F_{11} 4.312×10^{-10} PSI^{-2}	F_{22} 4.708×10^{-10} PSI^{-2}	F_{66} 5.476×10^{-9} PSI^{-2}

Interaction Terms (Based on Tables 8, 9, 10)	F_{12} 6.367×10^{-11} PSI^{-3}	F_{112} -5.320×10^{-16} PSI^{-3}	F_{122} -4.049×10^{-16} PSI^{-3}
	F_{166} 3.749×10^{-15} PSI^{-3}	F_{266} 3.543×10^{-15} PSI^{-3}	
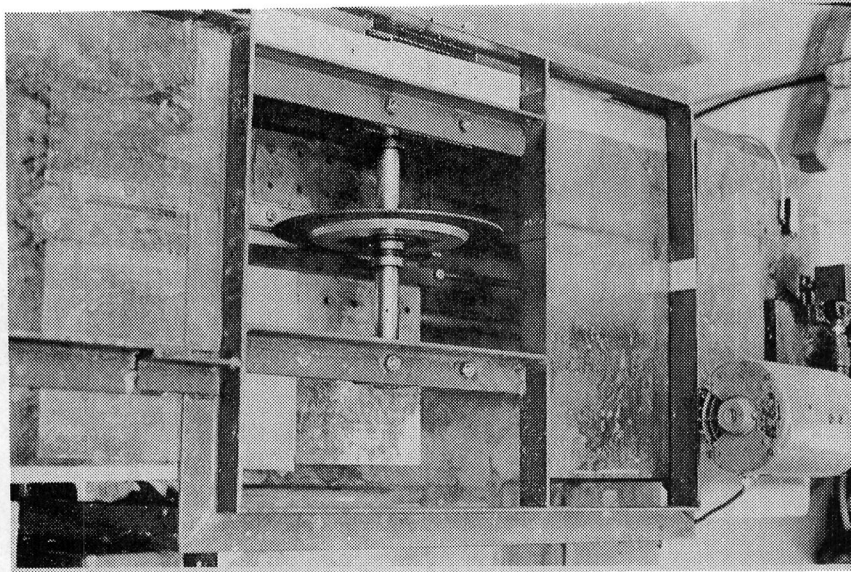
Fig. 1 FLAT SPECIMEN ABRASIVE WHEEL
CUTTING APPARATUS
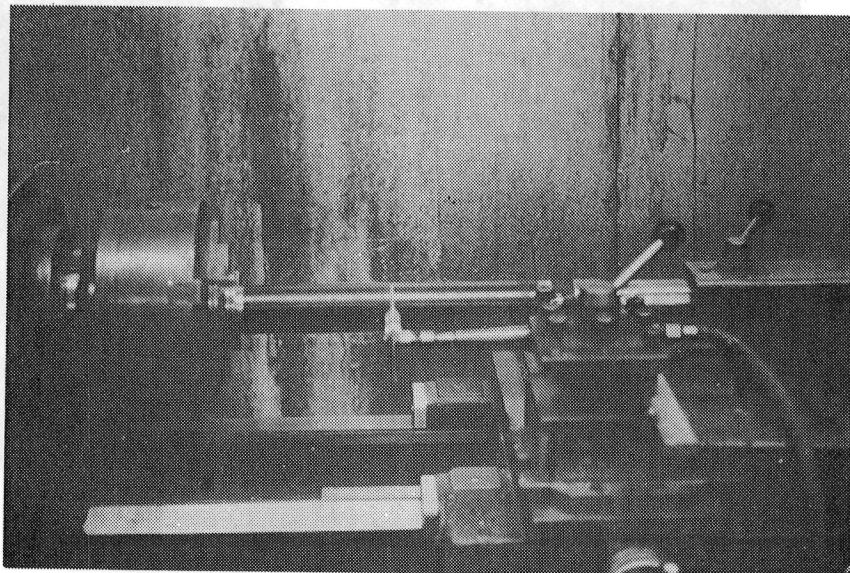
Fig. 2 TUBE CUTTING APPARATUS
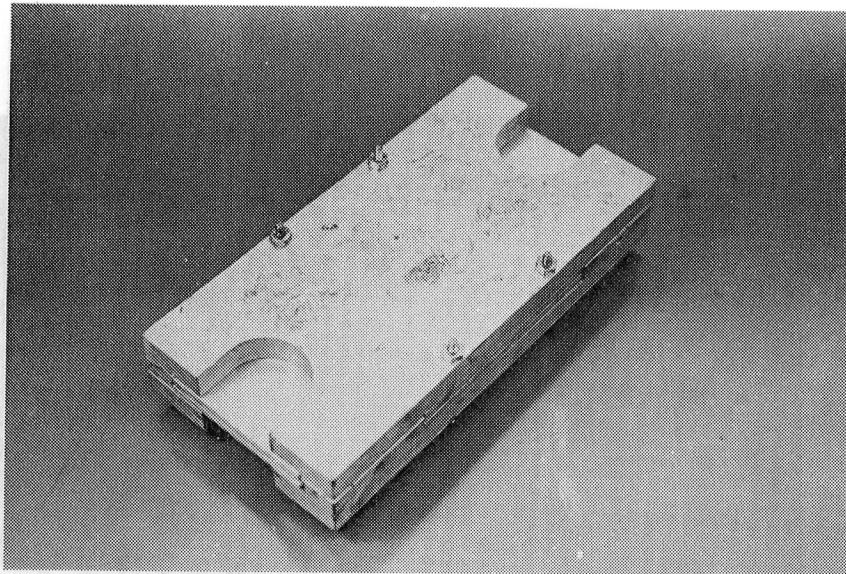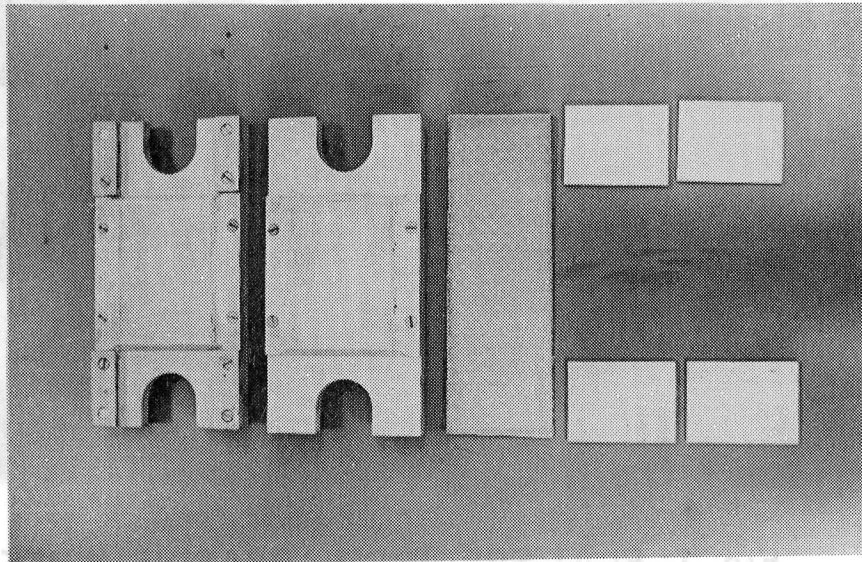
Fig. 3 TENSION SAMPLE and END GRIP FIXTURE
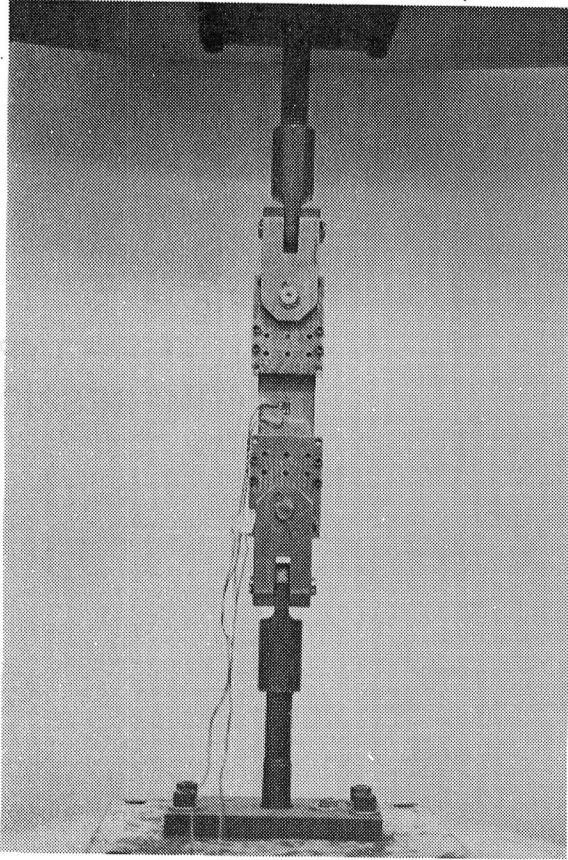
Fig. 4
TENSION GRIPS IN
TINIUS OLSEN
TESTING MACHINE
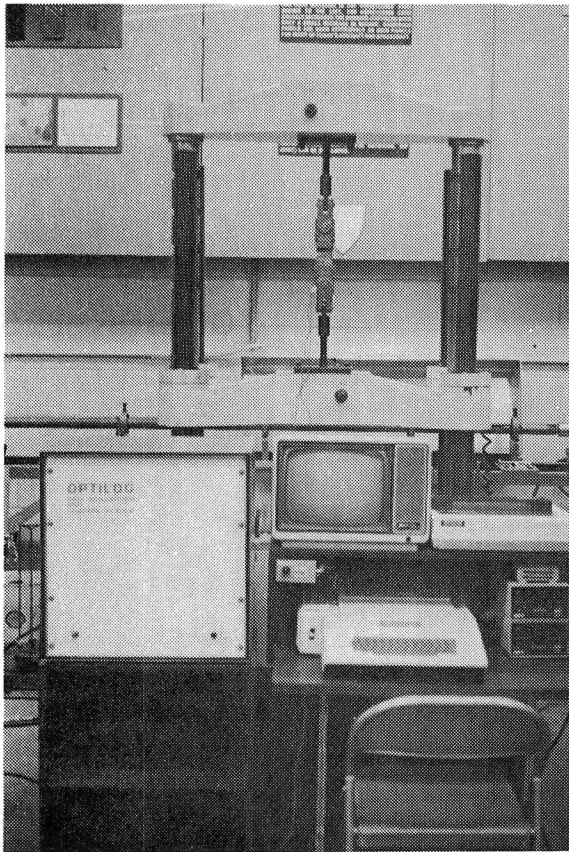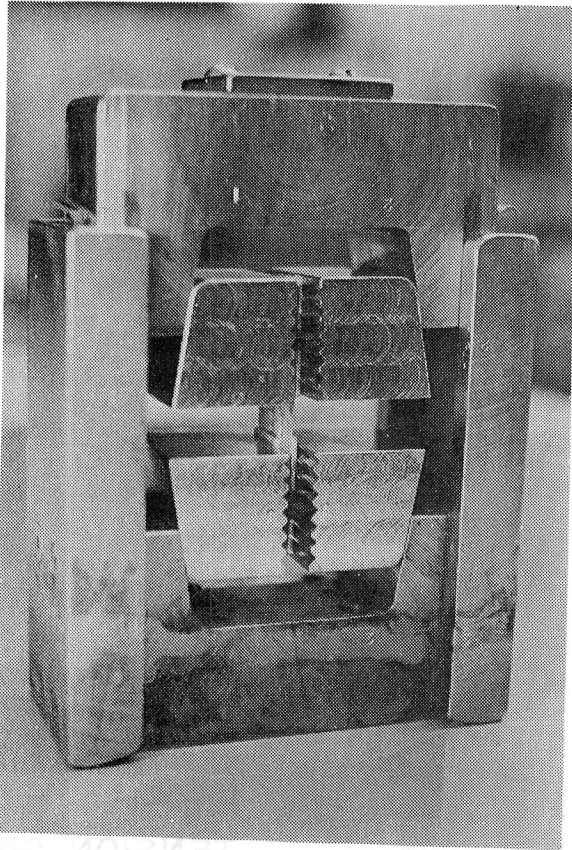
Fig. 5
II TRI – TYPE
COMPRESSION GRIPS
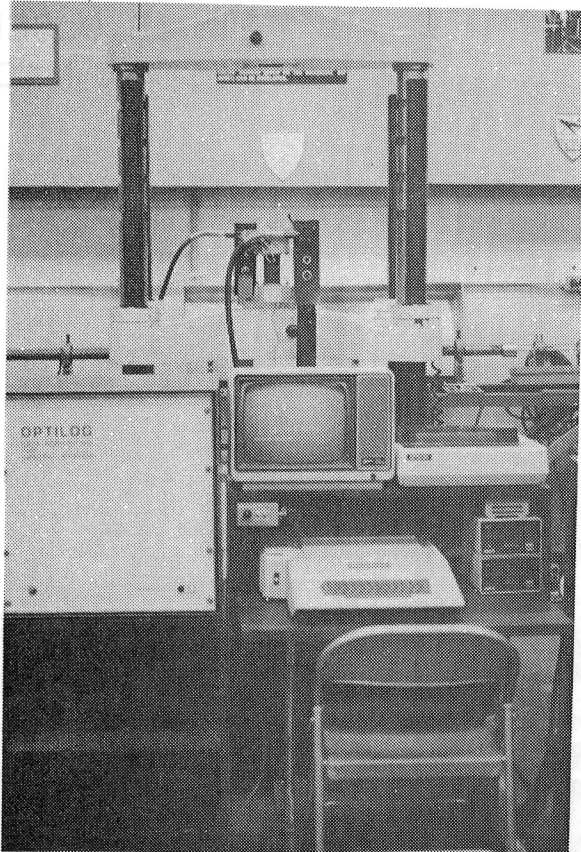
Fig. 6
TORSION TEST
FACILITY
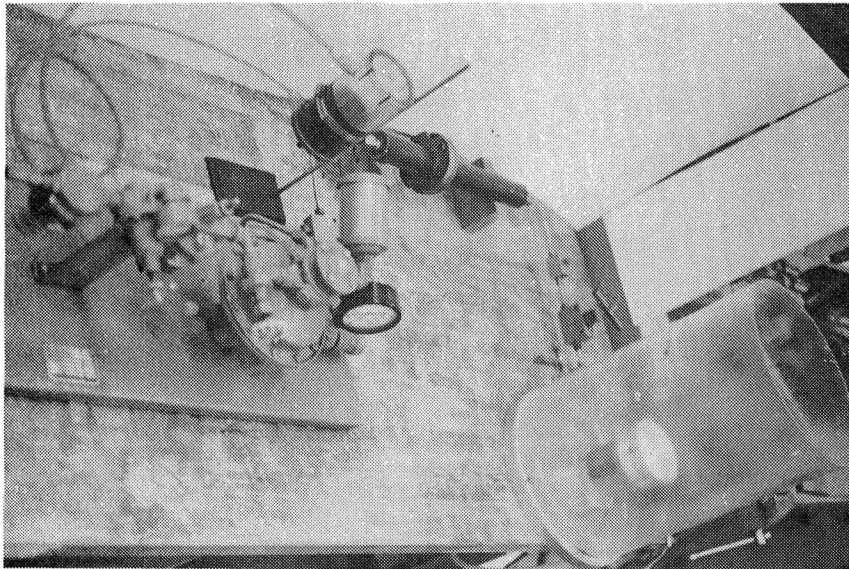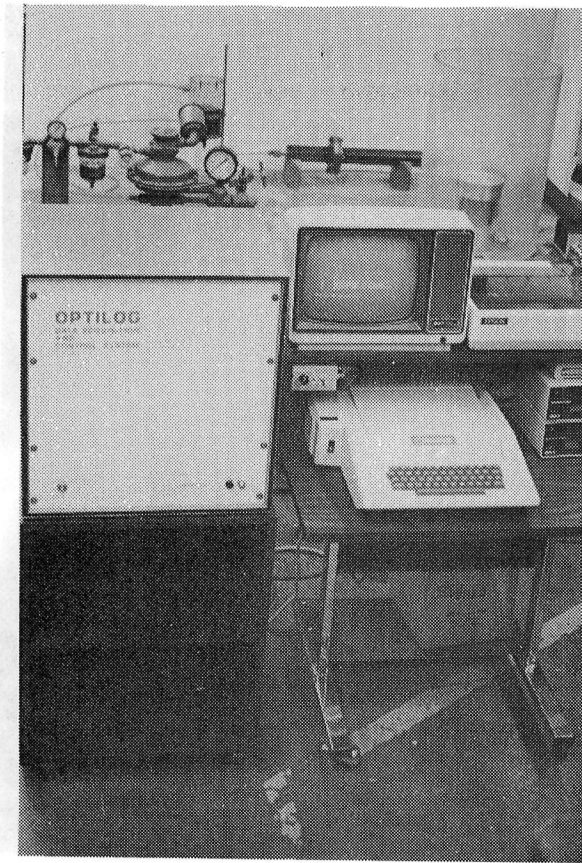
Fig. 7 PRESSURE TEST FACILITY WITH DATA
        ACQUISITION SYSTEM
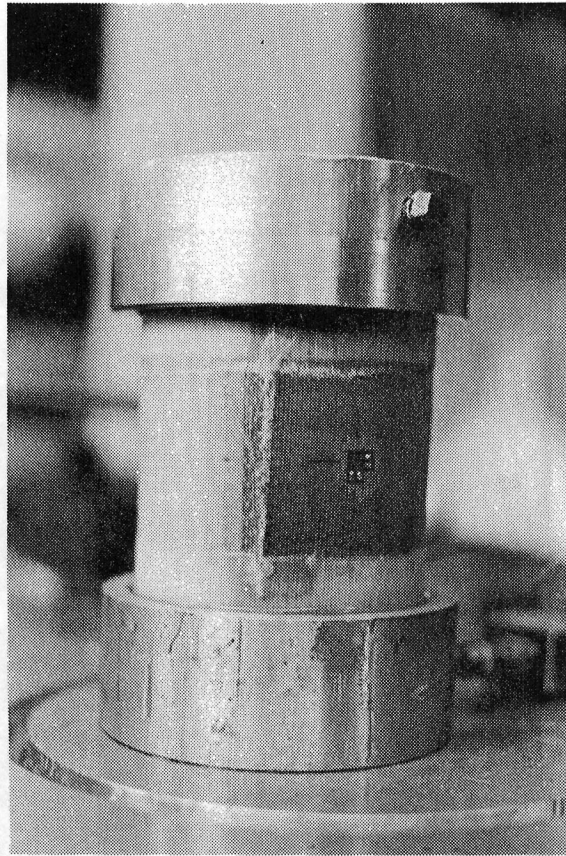
Fig. 8 PRESSURE TEST SPECIMEN
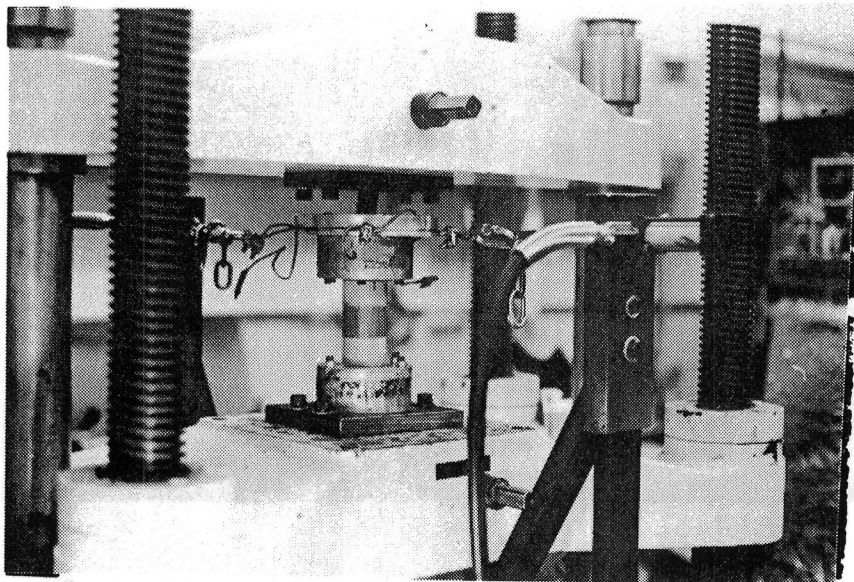
Fig. 9 TENSION - TORSION TEST APPARATUS

FIGURE 10 TENSION TEST
O DEG. KEVLAR WEAVE
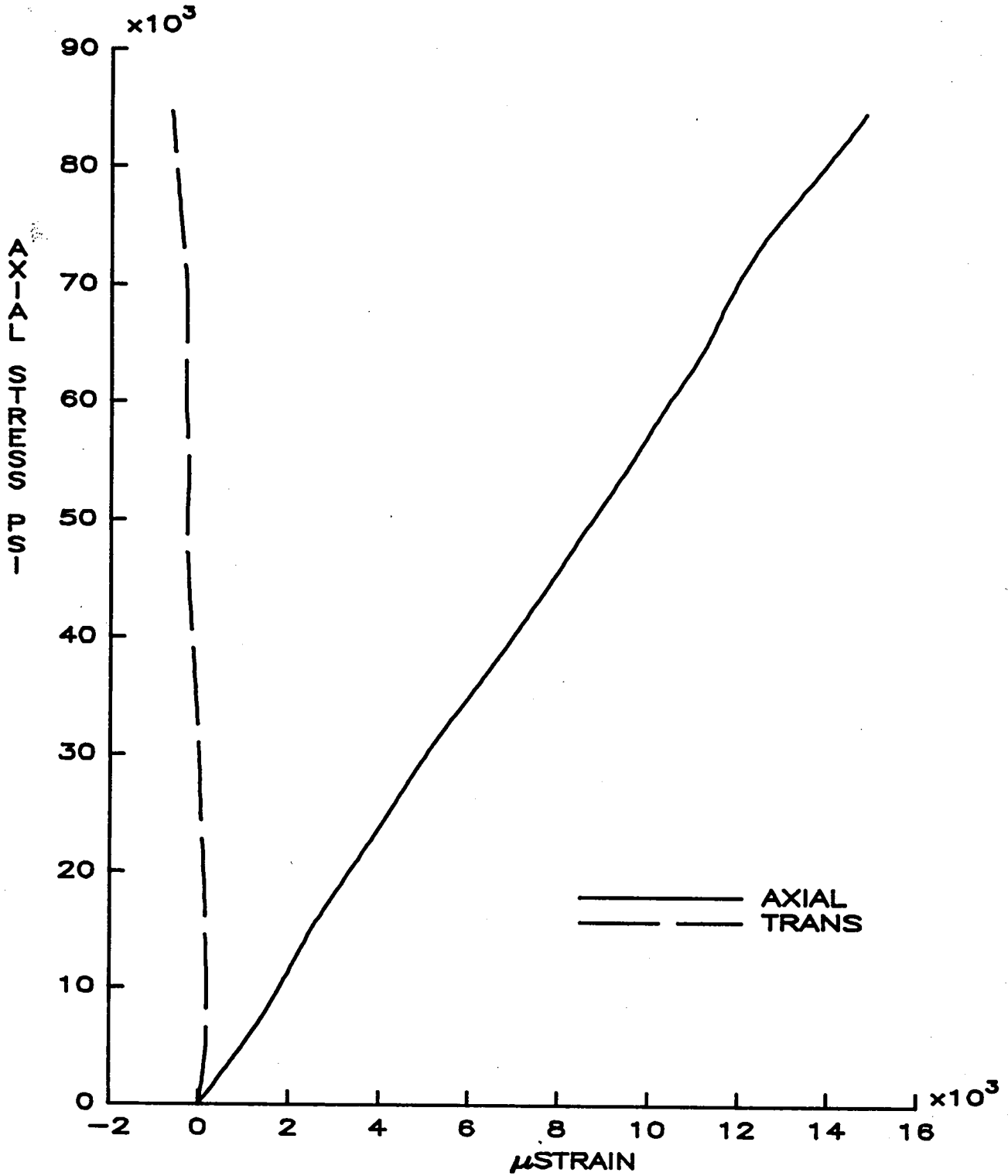
FIGURE 11 TENSION TEST
90 DEG. KEVLAR WEAVE
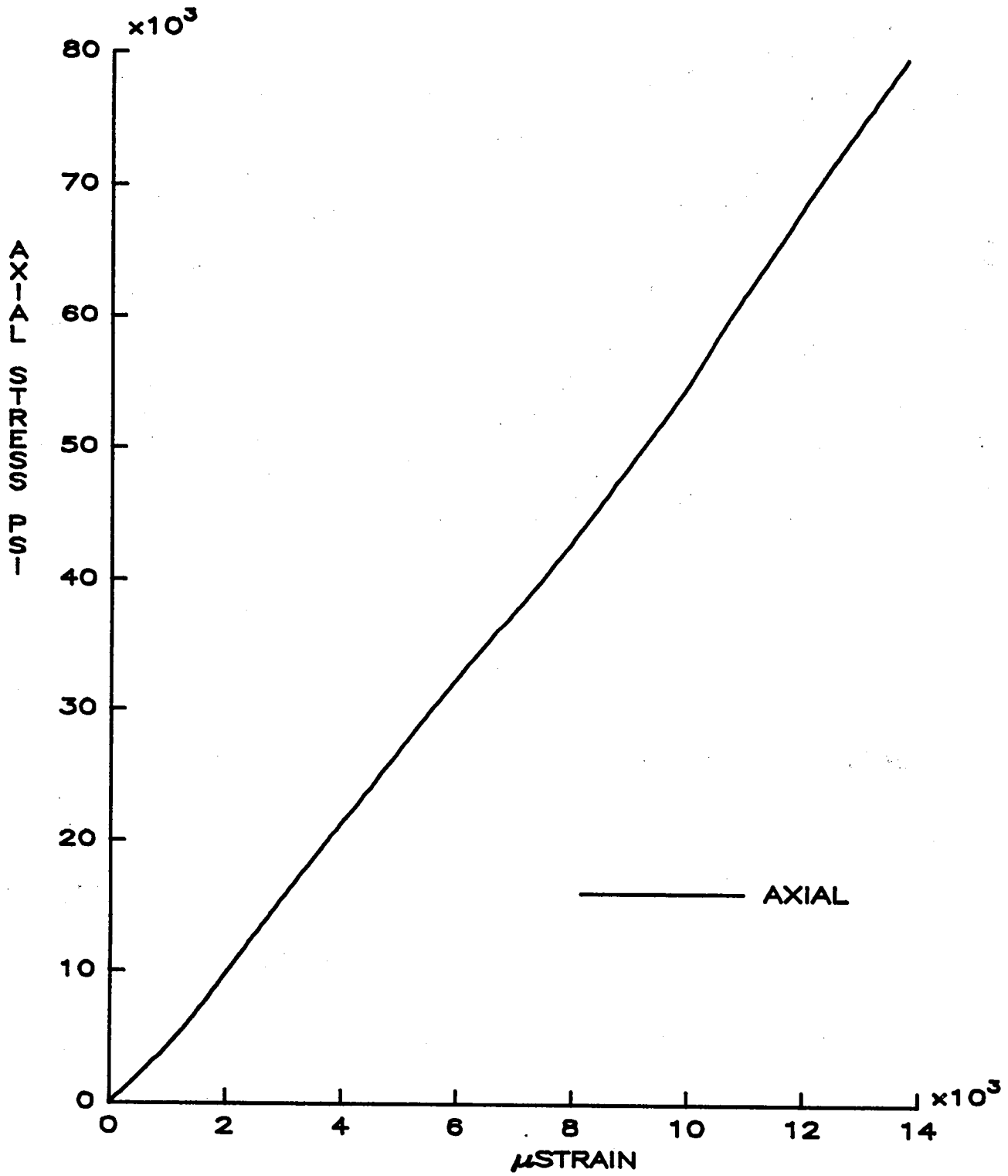
Fig. 12 90° STRENGTH vs MISALIGNMENT ANGLE
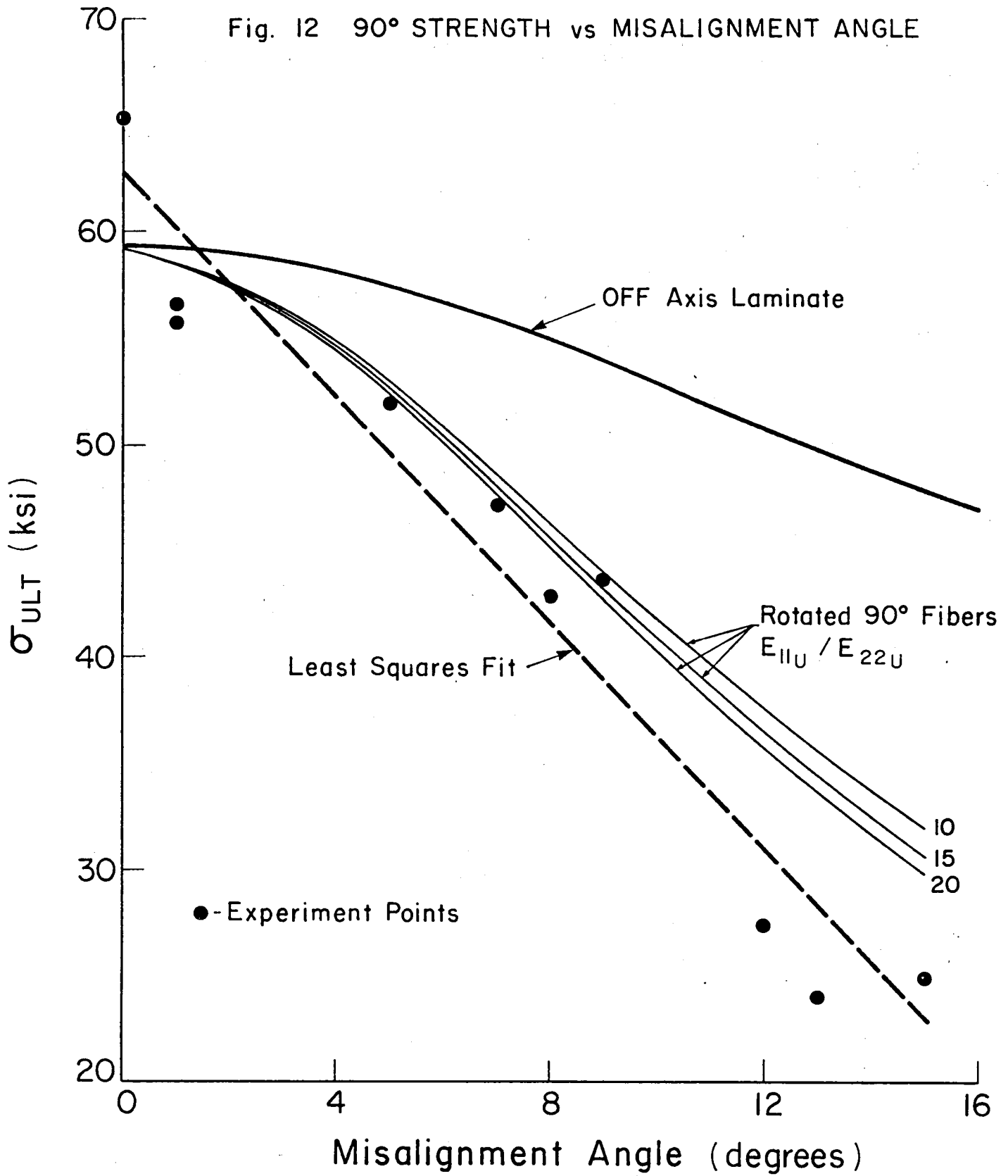
Fig. 13   90° MODULUS vs MISALIGNMENT ANGLE
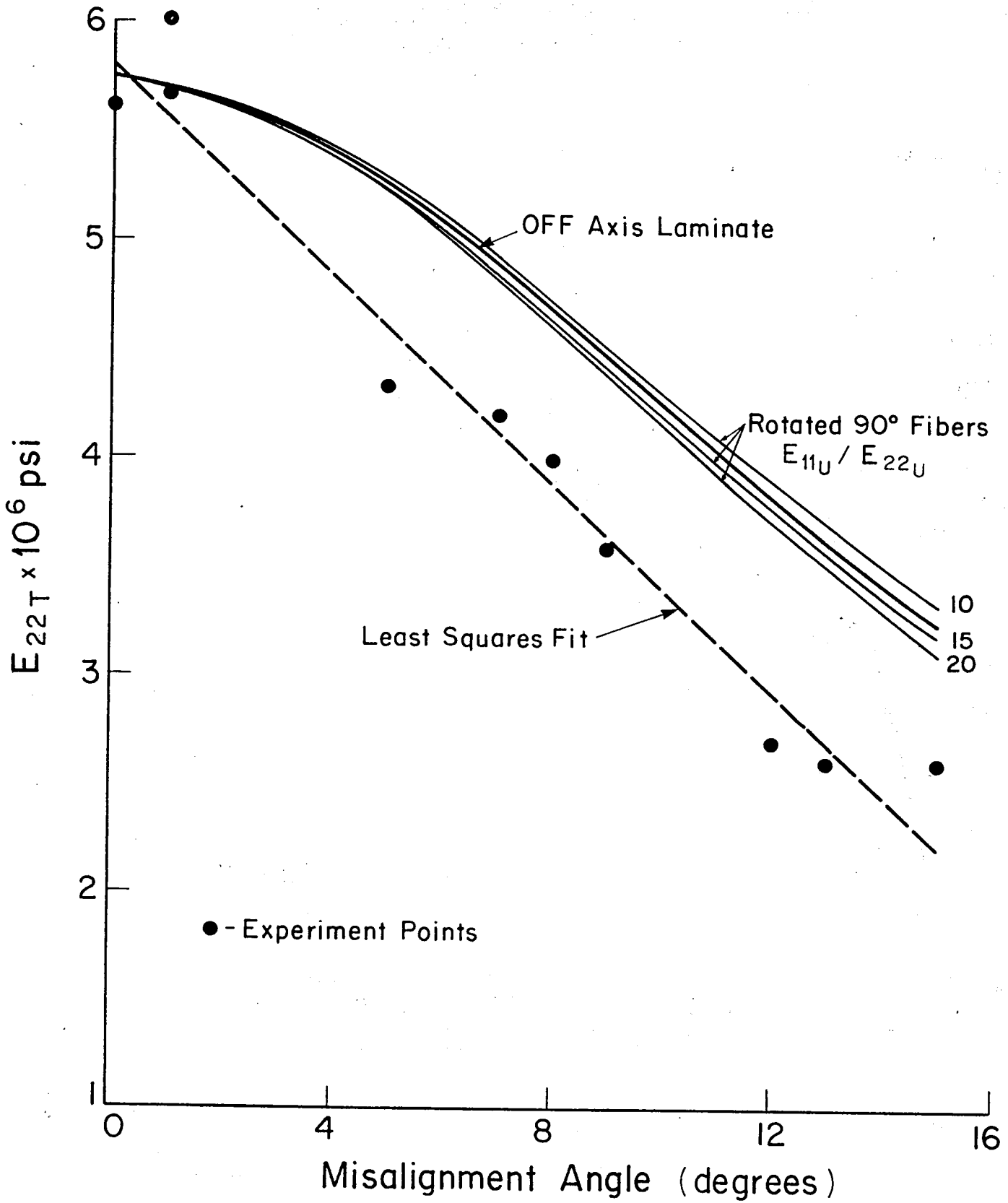
FIGURE 14 COMPRESSION TEST
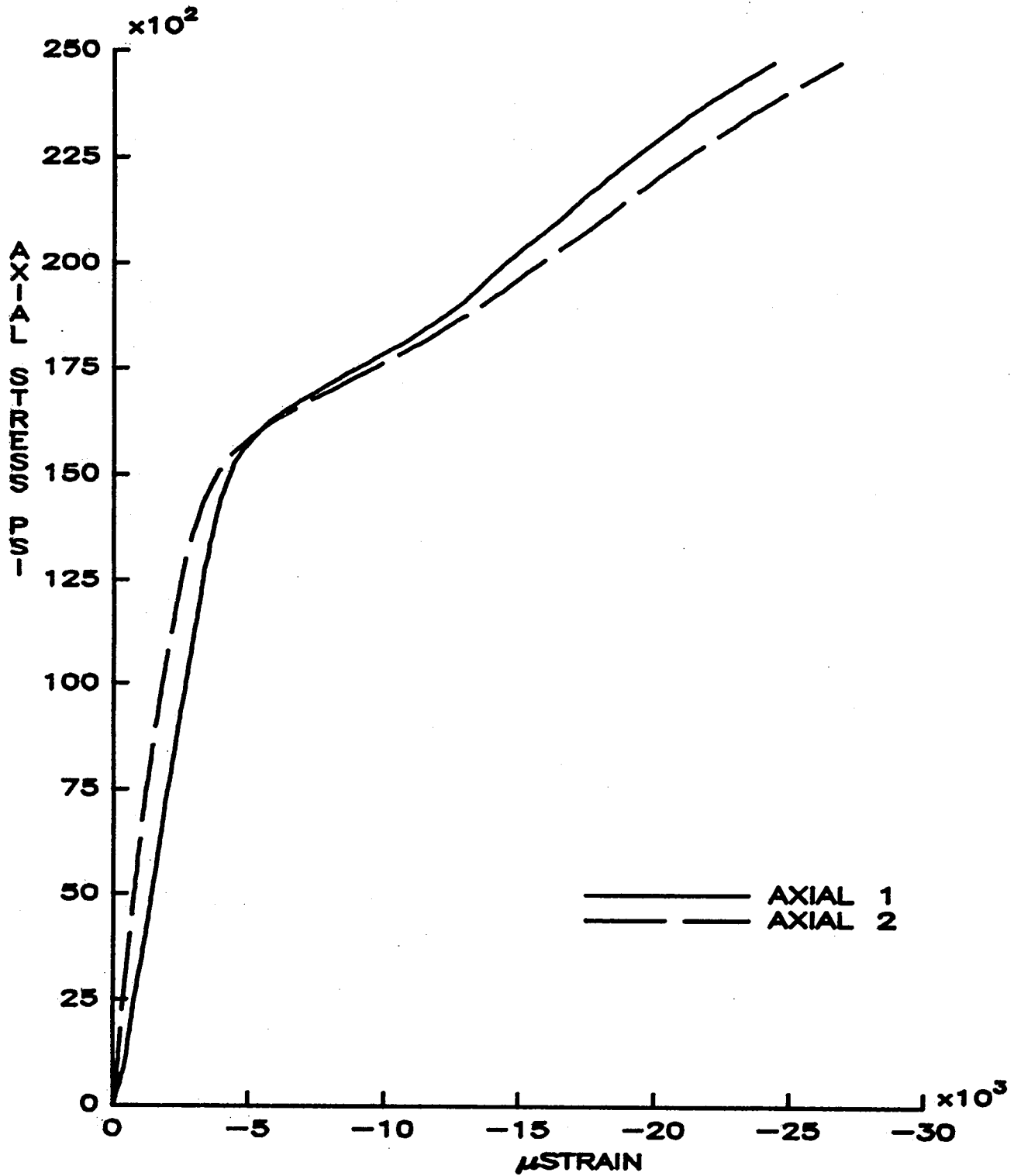O DEG. KEVLAR WEAVE
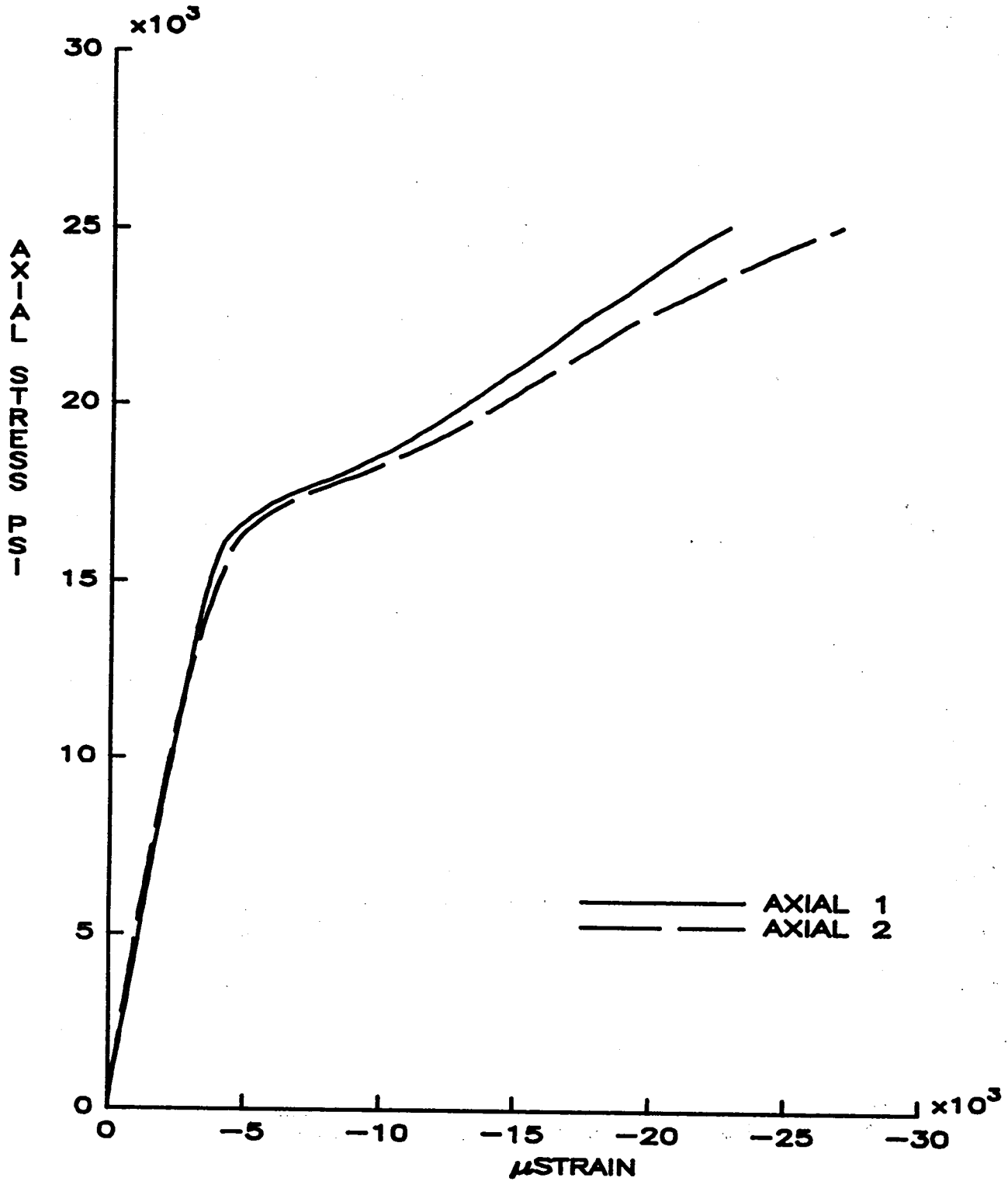
FIGURE 15 COMPRESSION TEST
90 DEG. KEVLAR WEAVE
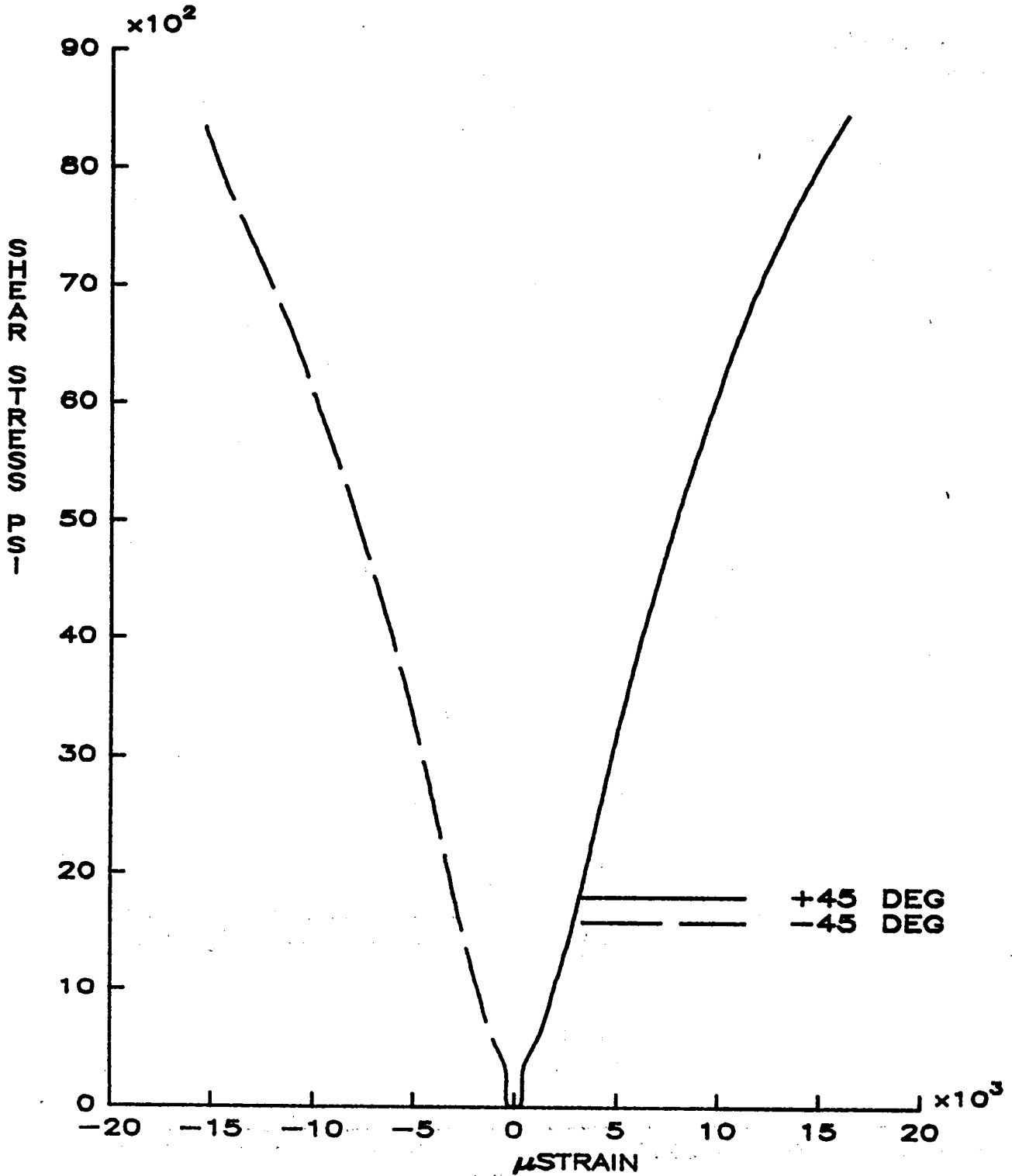
FIGURE 16 TORSION TEST
O DEG KEVLAR WEAVE
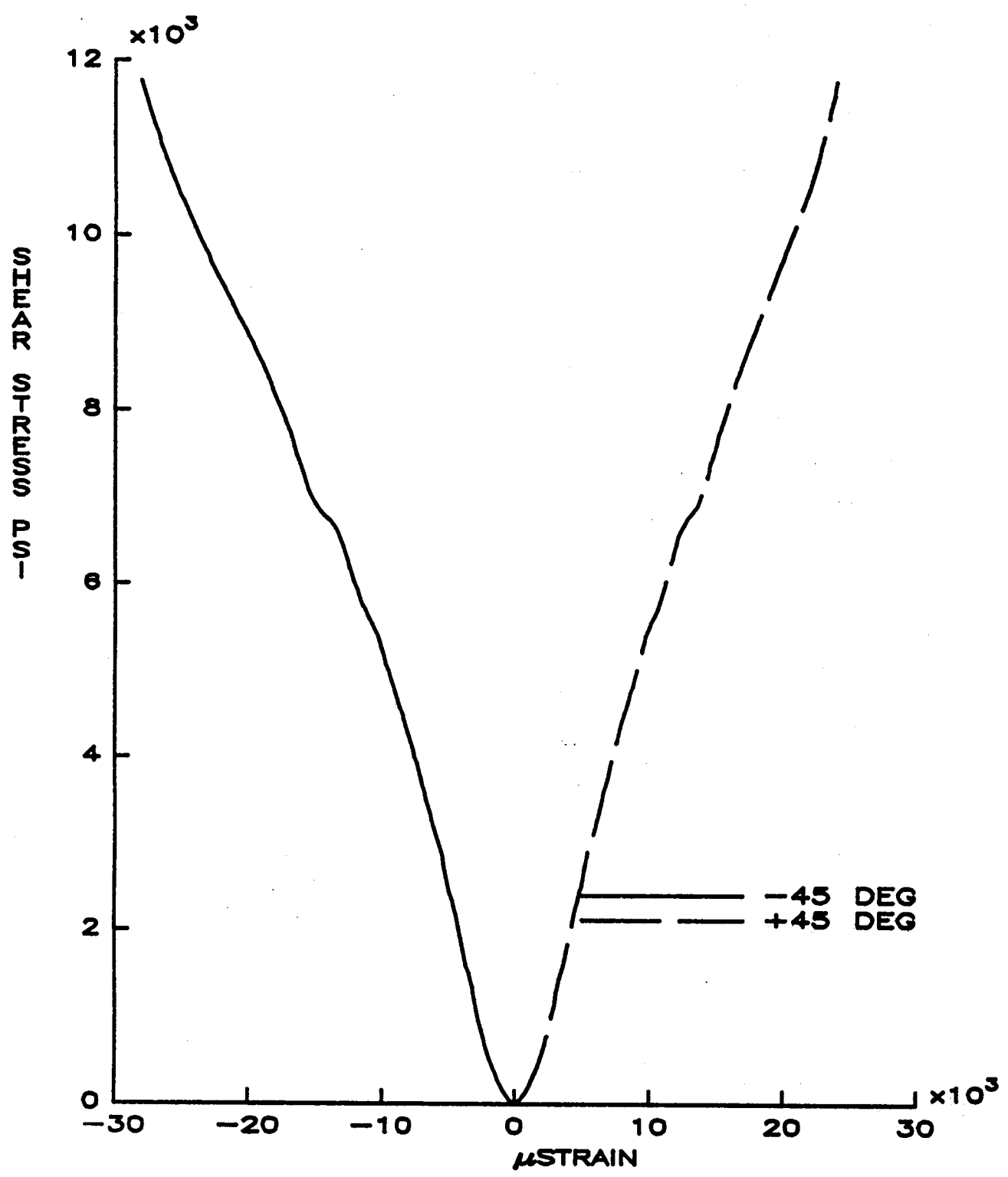
FIGURE 17 TORSION TEST
90 DEG. KEVLAR WEAVE

FIGURE 18 INTERNAL PRESSURE TEST
O DEG. KEVLAR WEAVE
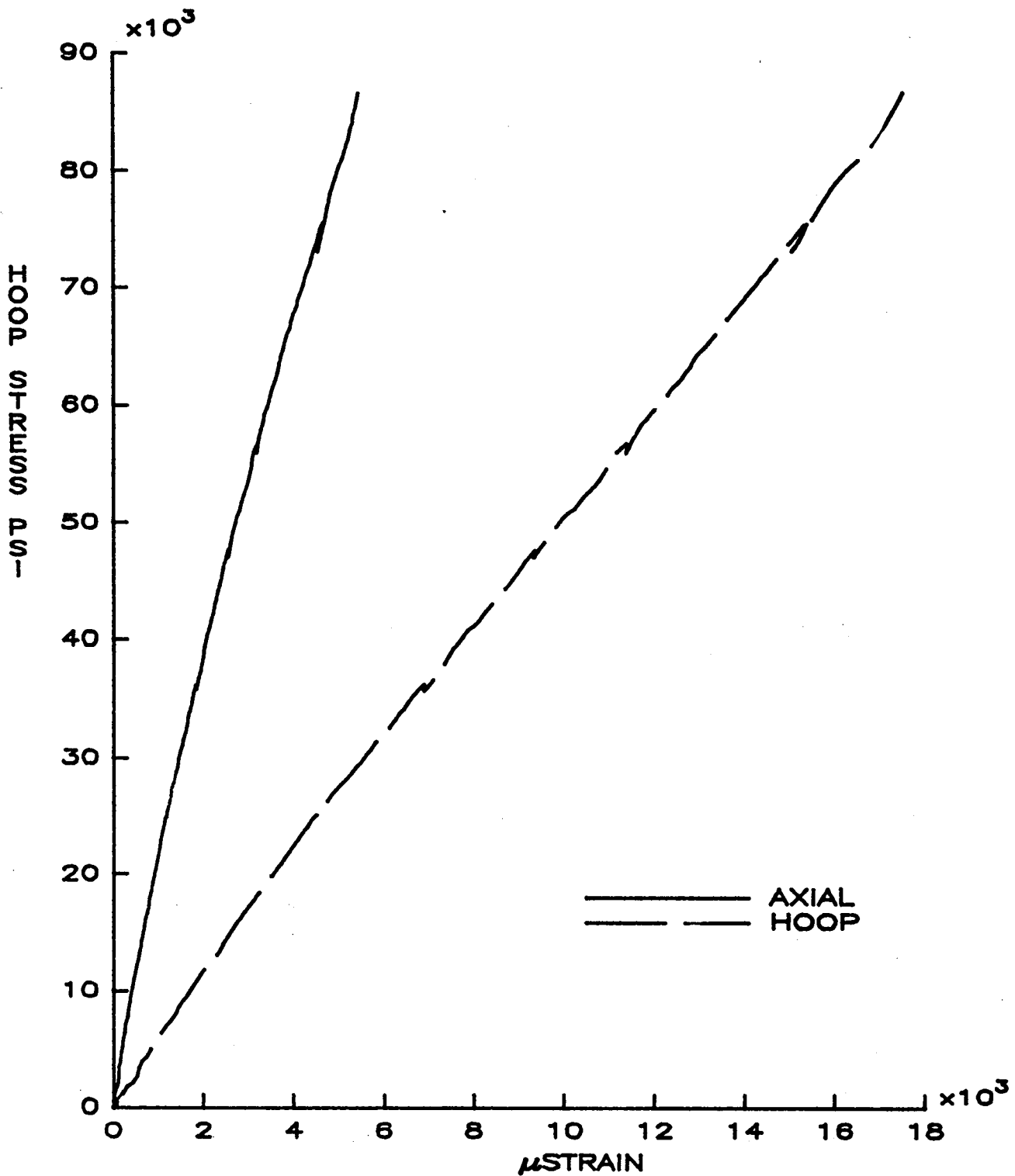AXIAL STRESS = HOOP STRESS / 2

FIGURE 19 INTERNAL PRESSURE TEST
90 DEG. KEVLAR WEAVE
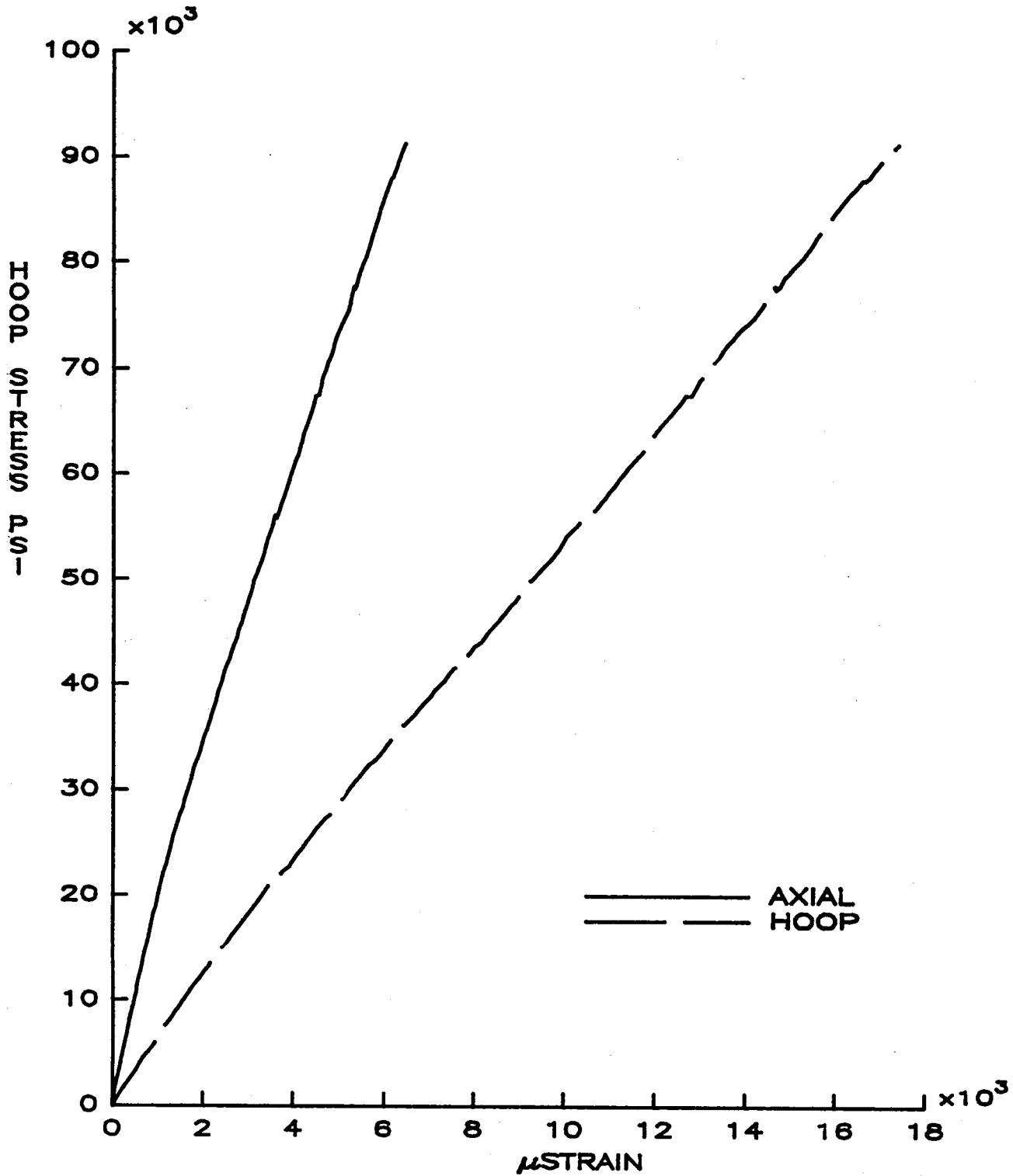AXIAL STRESS = HOOP STRESS / 2

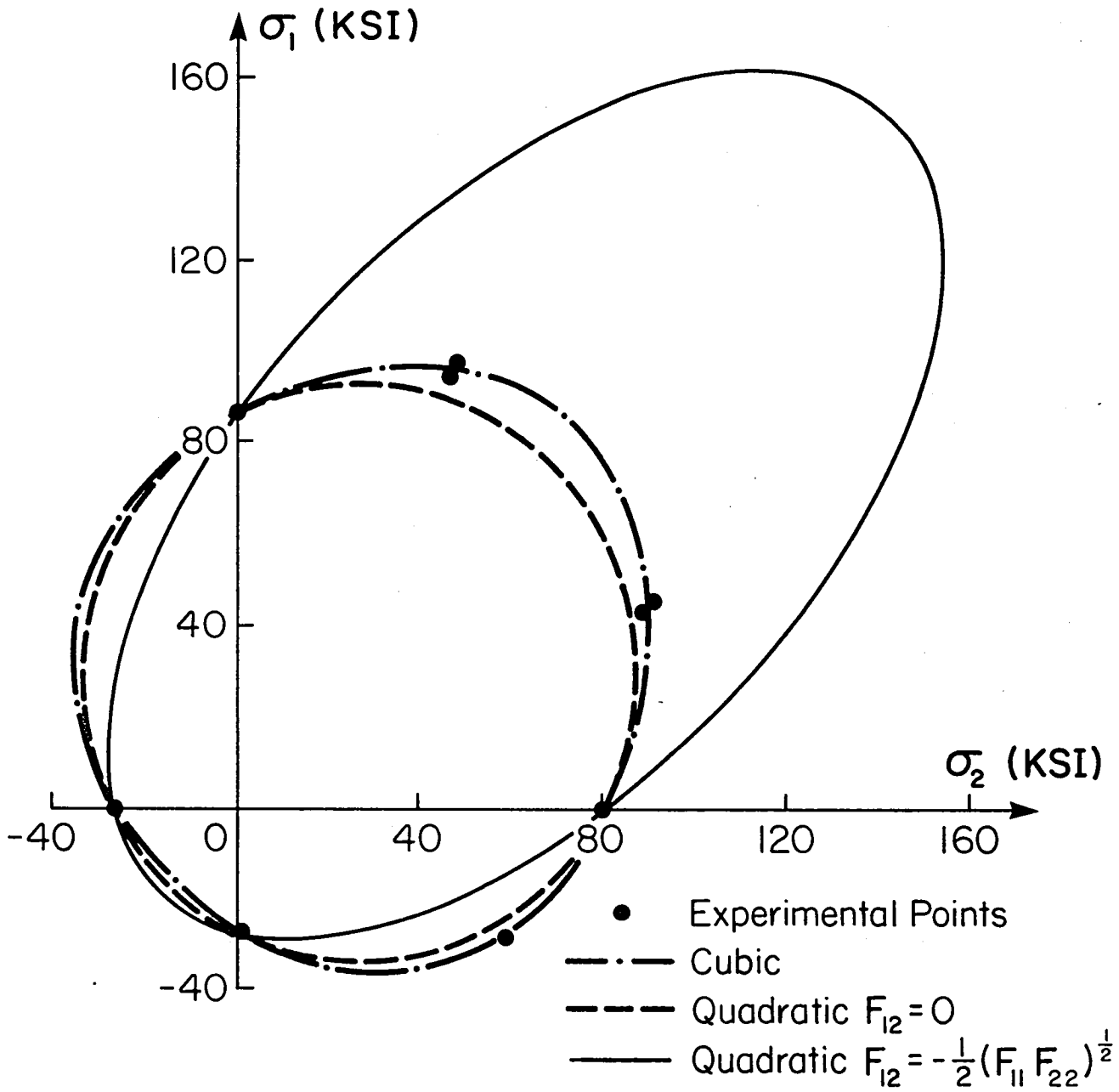Fig. 20 Comparison of Failure Models for $\sigma_6 = 0$
Woven Kevlar/Epoxy Fabric Prepreg Narmco 5208-K285

- Experimental Points
—·— Cubic
——— Quadratic $F_{12} = 0$
——— Quadratic $F_{12} = -\frac{1}{2}(F_{11} F_{22})^{\frac{1}{2}}$

Fig. 21

Fig. 22

$$\sigma_1 = R \cos \theta \sin \phi$$
$$\sigma_2 = R \sin \theta \sin \phi$$
$$\sigma_6 = R \cos \phi$$
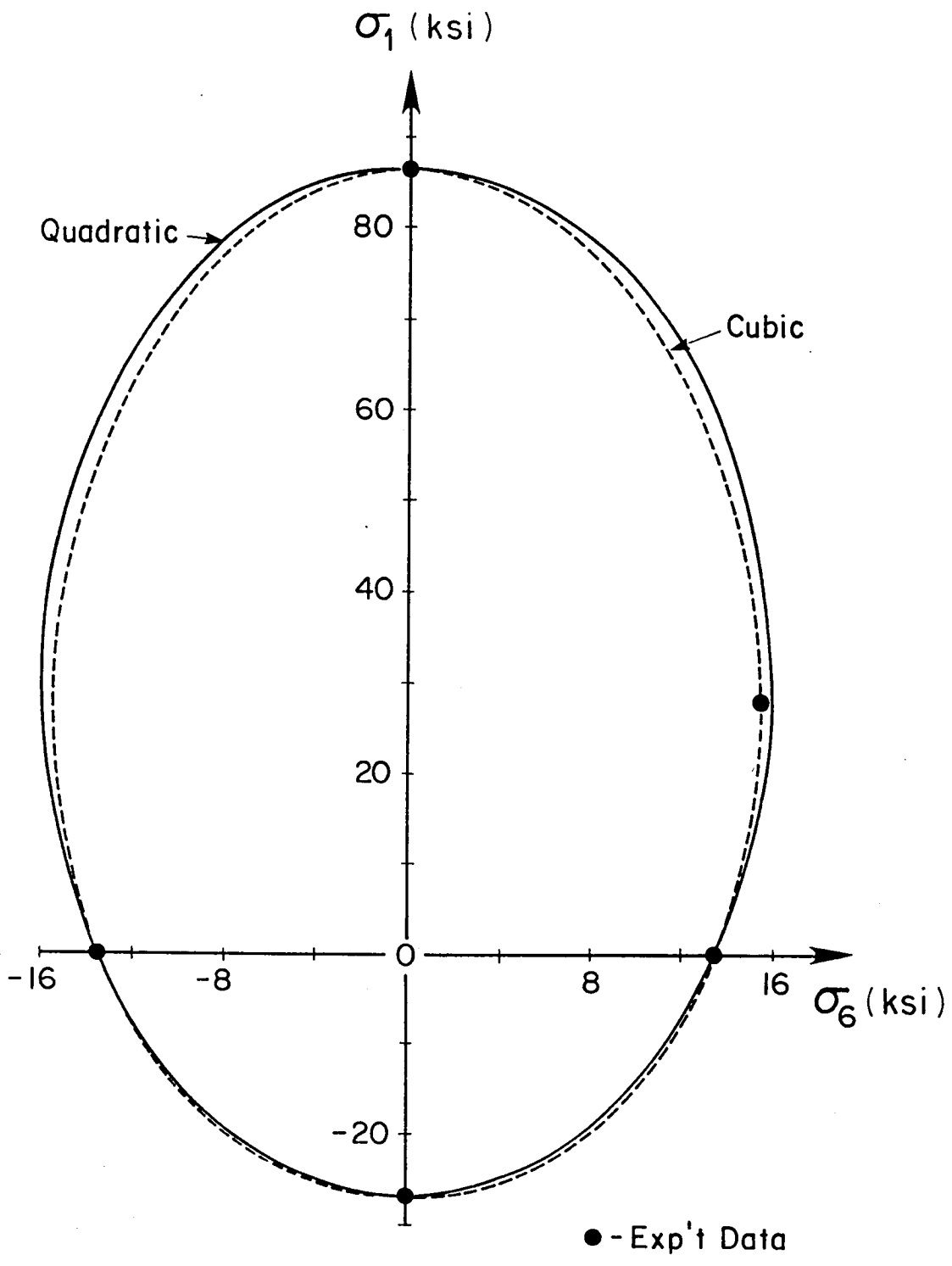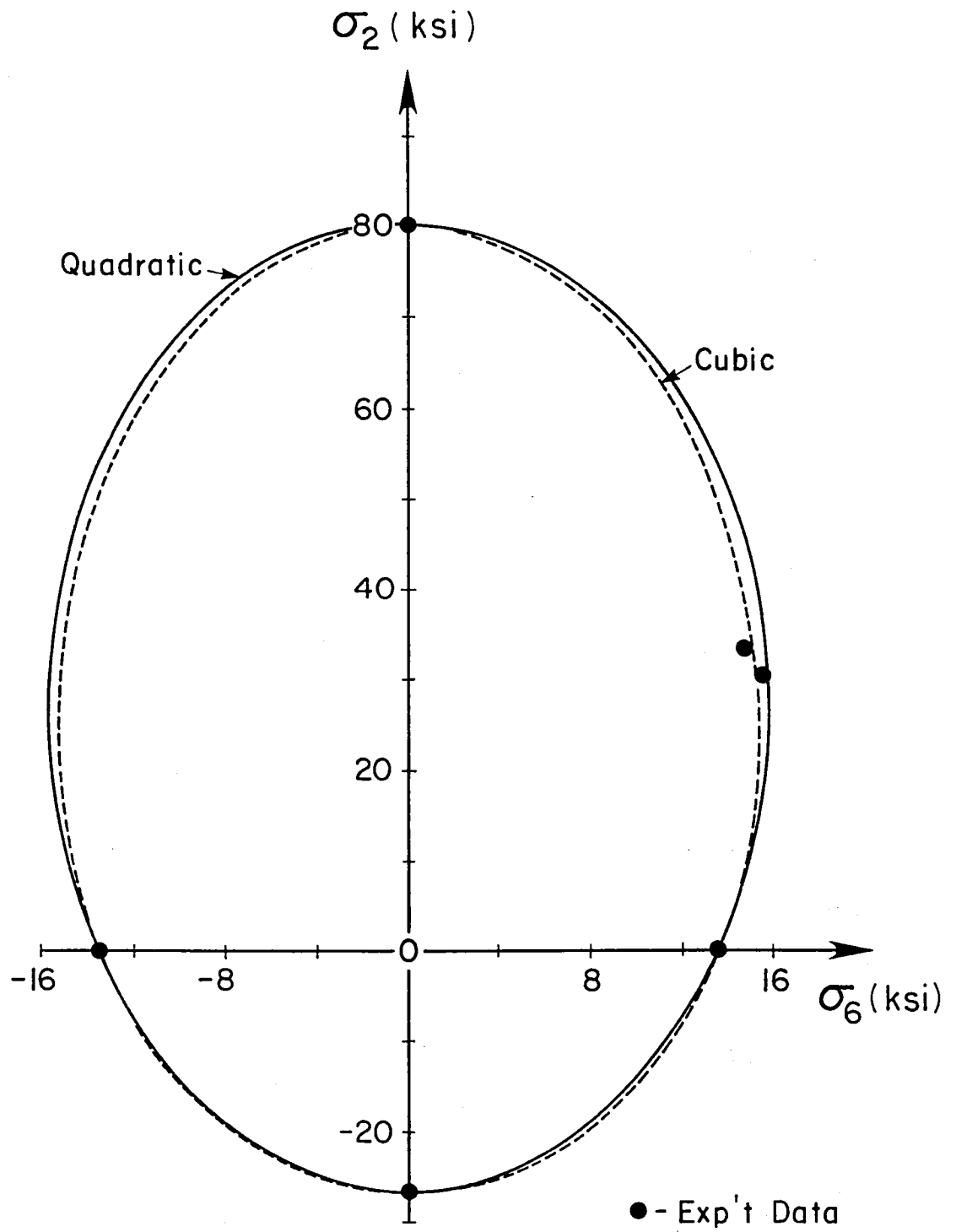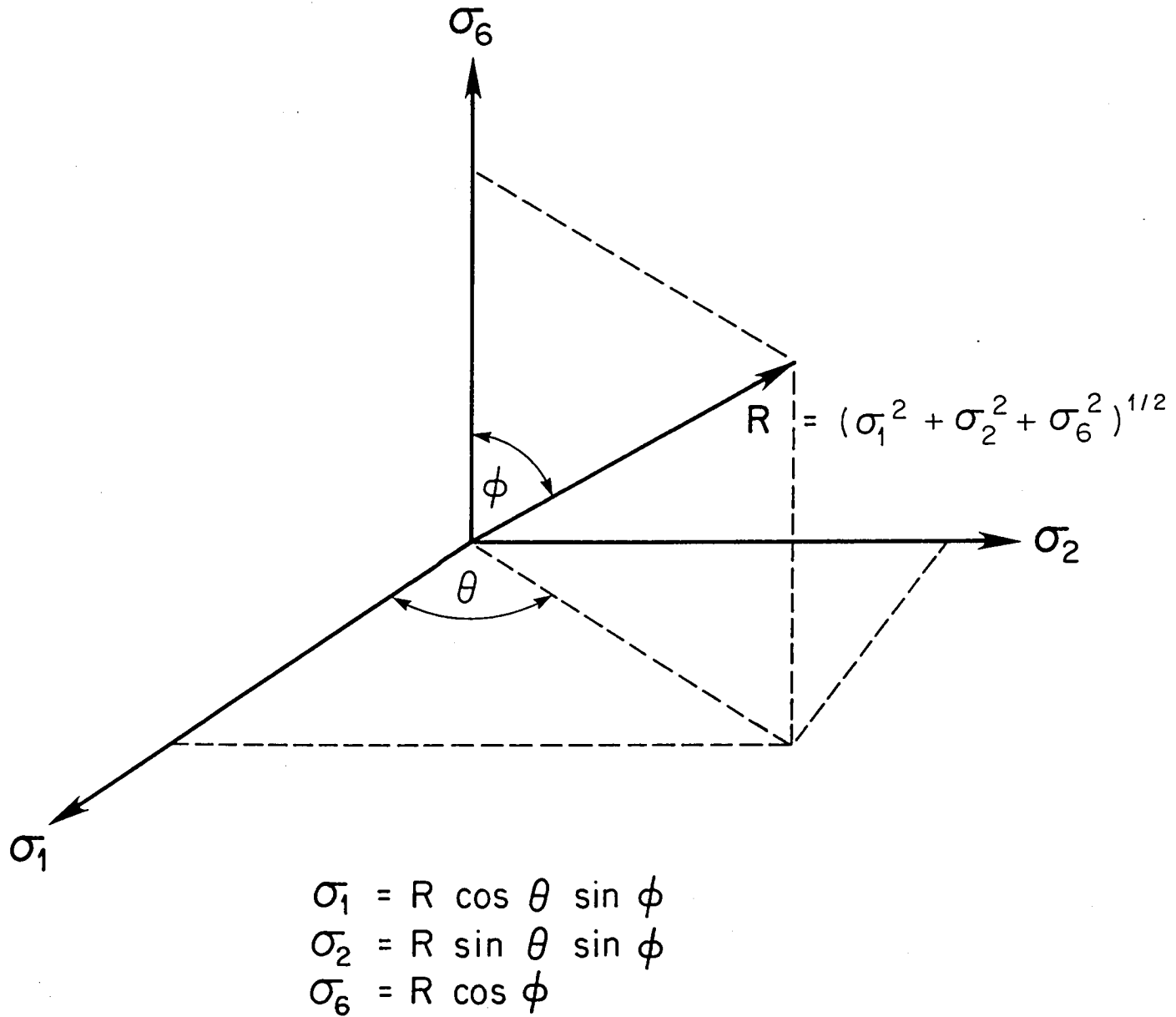
Fig. 23   RESOLUTION OF LOAD VECTOR R
IN STRESS SPACE

Fig. 24 Design Factors for Correcting Quadratic Model Strength Predictions
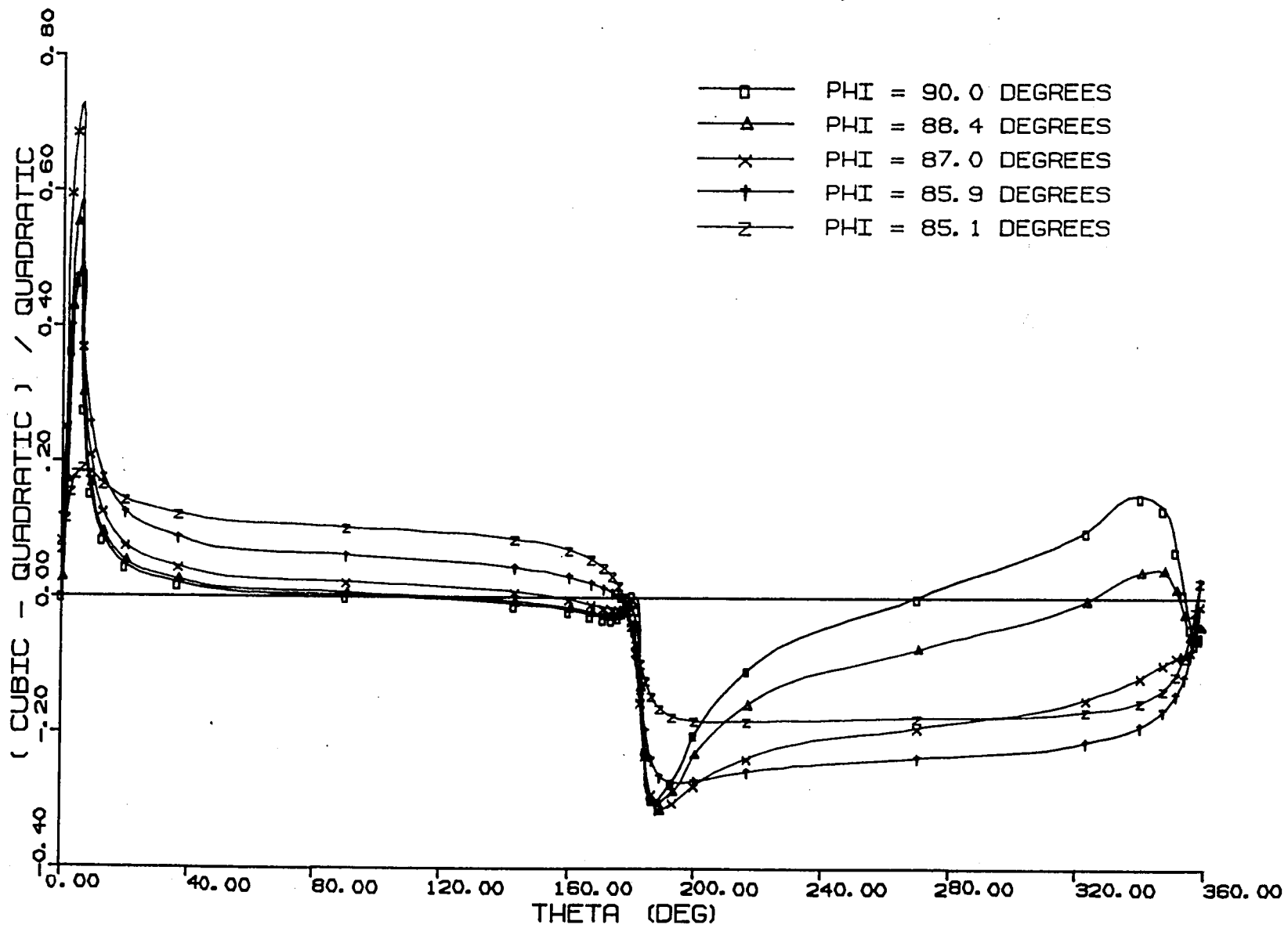(Plane Stress State)

51

Fig. 25   Design Factors for Correcting
Quadratic Model Strength Predictions
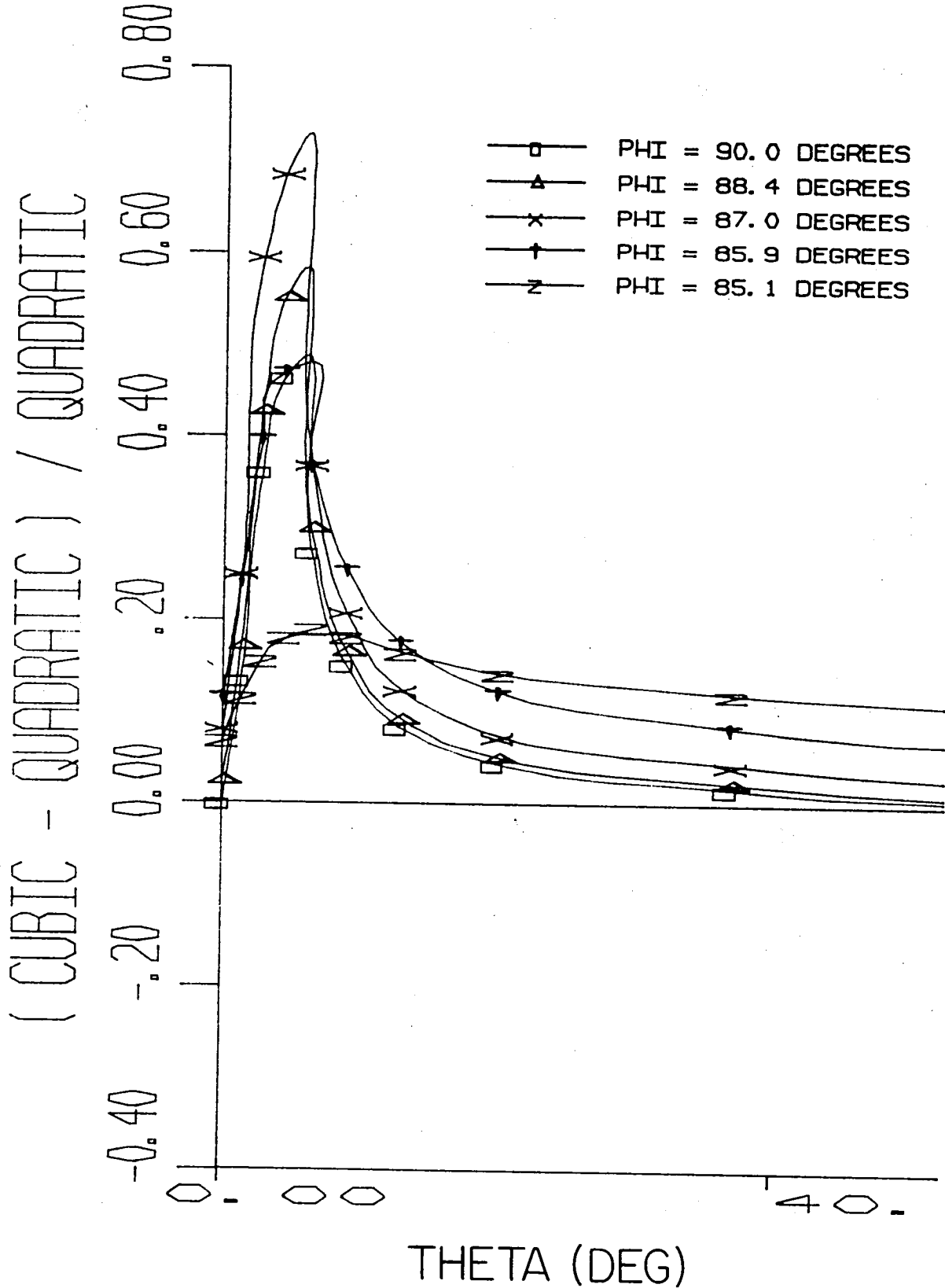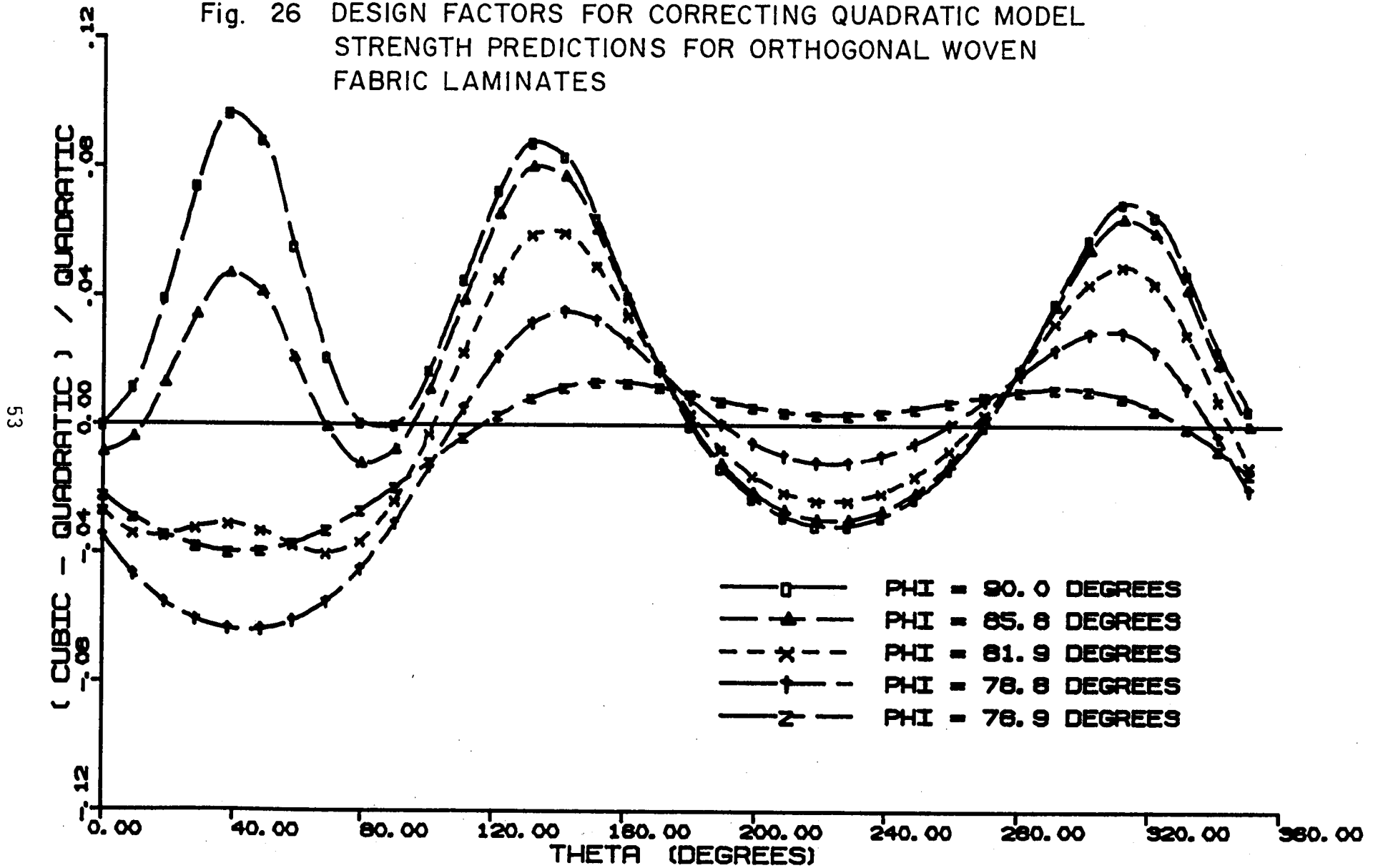(Plane Stress State)

52

Fig. 26 DESIGN FACTORS FOR CORRECTING QUADRATIC MODEL STRENGTH PREDICTIONS FOR ORTHOGONAL WOVEN FABRIC LAMINATES

APPENDIX: <u>STIFFNESS AND STRENGTH</u>

<u>ANALYSIS OF WOVEN MATERIALS</u>

In order to analyze the stress state in the composite material it is necessary to define the stiffness matrix [Q], where for a single ply, the relationship is,

$$[\sigma] = [Q][\varepsilon] \qquad (A.1)$$

Expanded in the material coordinate axes, this becomes

$$
\begin{bmatrix} \sigma_1 \\ \sigma_2 \\ \tau_{12} \end{bmatrix}
=
\begin{bmatrix} Q_{11} & Q_{12} & Q_{16} \\ Q_{12} & Q_{22} & Q_{26} \\ Q_{16} & Q_{26} & Q_{66} \end{bmatrix}
\begin{bmatrix} \varepsilon_1 \\ \varepsilon_2 \\ \gamma_{12} \end{bmatrix}
\qquad (A.2)
$$

If one considers the weave material to consist of two separate materials superimposed on top of each other, equation (A.2) becomes,

$$
\begin{bmatrix} \sigma_1 \\ \sigma_2 \\ \tau_{12} \end{bmatrix}
=
\left\{
\begin{bmatrix} Q'_{11} & Q'_{12} & Q'_{16} \\ Q'_{12} & Q'_{22} & Q'_{26} \\ Q'_{16} & Q'_{26} & Q'_{66} \end{bmatrix}
+
\begin{bmatrix} Q''_{11} & Q''_{12} & Q''_{16} \\ Q''_{12} & Q''_{22} & Q''_{26} \\ Q''_{16} & Q''_{26} & Q''_{66} \end{bmatrix}
\right\}
\begin{bmatrix} \varepsilon_1 \\ \varepsilon_2 \\ \gamma_{12} \end{bmatrix}
\qquad (A.3)
$$

where the ' and " represent the two directions of fibers (i.e.: warp and fill). It is now necessary to define the new [Q¹] and [Q¹¹] matrices in terms of known properies of the material. Since one set of fibers is usually straight, one can then define the '1' direction to be parallel to

the straight fibers. The [Q'] matrix will represent the contribution due to the straight (warp direction) fibers and the [Q"] matrix will represent the contribution from the 'fill' direction fibers.

For a general unidirection material the stiffness terms are, (in the material coordinates)

$$Q_{11_u} = \frac{E_{11_u}}{1-\nu_{12_u}\nu_{21_u}}$$

$$Q_{22_u} = \frac{E_{22_u}}{1-\nu_{12_u}\nu_{21_u}} \qquad\qquad (A.4)$$

$$Q_{12_u} = \frac{\nu_{12_u}E_{22_u}}{1-\nu_{12_u}\nu_{21_u}}$$

$$Q_{66_u} = G_{12_u}$$

$$Q_{16_u} = 0$$

$$Q_{26_u} = 0$$

where the subscript 'u' denotes 'unidirectional'. If we rotate the unidirectional ply by some angle $\emptyset$ with respect to the structual axes, one obtains

$$Q_{11} = Q_{11_u}\cos^4\emptyset + 2(Q_{12_u} + 2Q_{66_u})\ \sin^2\emptyset\cos^2\emptyset + Q_{22}\sin^4\emptyset$$

$$Q_{22} = Q_{11_u}\sin^4\emptyset + 2(Q_{12_u} + 2Q_{66_u})\ \sin^2\emptyset\cos^2\emptyset + Q_{22}\cos^4\emptyset$$

$$\hat{Q}_{12} = (Q_{11_u} + Q_{22_u} - 4Q_{66_u})\sin^2\!\emptyset\cos^2\!\emptyset + Q_{12_u}(\sin^4\!\emptyset + \cos^4\!\emptyset) \qquad (A.5)$$

$$\hat{Q}_{66} = (Q_{11_u} + Q_{22_u} - 2Q_{12_u} - 2Q_{66_u})\sin^2\!\emptyset\cos^2\!\emptyset + Q_{66_u}(\sin^4\!\emptyset + \cos^4\!\emptyset)$$

$$\hat{Q}_{16} = (Q_{11_u} - Q_{12_u} - 2Q_{66_u})\sin\!\emptyset\cos^3\!\emptyset + (Q_{12_u} - Q_{22_u} + 2Q_{66_u})\sin^3\!\emptyset \quad \cos\!\emptyset$$

$$\hat{Q}_{26} = (Q_{11_u} - Q_{12_u} - 2Q_{66_u})\sin^3\!\emptyset\cos\!\emptyset + (Q_{12_u} - Q_{22_u} + 2Q_{66_u})\sin\!\emptyset\cos^3\!\emptyset$$

One can now equate [Q'] to equation (A.4) and [Q"] to equation A.5 where the material properties E_{11_u}, E_{22_u}, ν_{12_u}, ν_{21_u}, and G_{12_u} are for one set of fibers only, and $\emptyset = 90° + \alpha$, where α is the 'misalignment' angle. All that remains is to define the properties of the unidirectional material. Consider now the case where the 90° fibers are square to the 0° fibers, then $\emptyset = 90°$ and solving for [Q"] gives,

$$Q''_{11} = Q_{22_u}$$

$$Q''_{22} = Q_{11_u}$$

$$Q''_{12} = Q_{12_u} \qquad (A.6)$$

$$Q''_{66} = Q_{66_u}$$

$$Q''_{16} = 0$$

$$Q''_{26} = 0$$

and for [Q'],

$$Q'_{11} = Q_{11_u}$$

$$Q'_{22} = Q_{22_u}$$

$$Q'_{12} = Q_{12_u} \qquad\qquad (A.7)$$

$$Q'_{66} = Q_{66_u}$$

$$Q'_{16} = 0$$

$$Q'_{26} = 0$$

Since in this case one can solve for $[Q_m]$, (where subscript m denotes the overall material stiffness matrix), from known material properties, one finds that,

$$Q_{11_m} = \frac{E_{11}}{(1-\nu_{12}\nu_{21})}$$

$$Q_{22_m} = \frac{E_{22}}{(1-\nu_{12}\nu_{21})} \qquad\qquad (A.8)$$

$$Q_{12_m} = \frac{\nu_{12}E_{11}}{(1-\nu_{12}\nu_{21})}$$

$$Q_{66_m} = G_{12}$$

$$Q_{16_m} = 0$$

$$Q_{26_m} = 0$$

Subtituting for $[Q_m] = [Q'] + [Q'']$ gives

$$Q_{11_m} = Q'_{11} + Q''_{11}$$

$$Q_{22_m} = Q'_{22} + Q''_{22} \qquad\qquad (A.9)$$

$$Q_{12_m} = Q'_{12} + Q''_{12}$$

$$Q_{66_m} = Q'_{66} + Q''_{66}$$

Next, substituting equations (A.7) and (A.8) into (A.9) gives

$$Q_{11_m} = Q_{11_u} + Q_{22_u}$$

$$Q_{22_m} = Q_{22_u} + Q_{11_u} \qquad\qquad (A.10)$$

$$Q_{12_m} = Q_{12_u} + Q_{12_u}$$

$$Q_{66_m} = Q_{66_u} + Q_{66_u}$$

From these relations one finds $Q_{12_u} = \dfrac{Q_{12_m}}{2}$ and $Q_{66_u} = \dfrac{Q_{66_m}}{2}$ and $Q_{11_m} = Q_{22_m} =$

$Q_{11_u} + Q_{22_u}$. Since Q_{11_u} and Q_{22_u} have not been measured, one can assume for

purposes of illustration a ratio of $\dfrac{Q_{11_u}}{Q_{22_u}} = K$, where K is determined from

stiffness values of unidirectional material, such as Kevlar/Epoxy for

59

example. This gives the resultant unidirectional values as,

$$Q_{11_u} = \frac{K}{K+1} Q_{11_m}$$

$$Q_{22_u} = \frac{1}{K+1} Q_{11_m} \qquad\qquad (A.11)$$

$$Q_{12_u} = \frac{Q_{12_m}}{2}$$

$$Q_{66_u} = \frac{Q_{66_m}}{2}$$

This assumes that the material modulus is the same in the two fiber directions. If this is not true, then equation (A.10) is rewritten as,

$$Q_{11_m} = Q_{11_u}0 + Q_{11_u}90$$

$$Q_{22_m} = Q_{22_u}0 + Q_{22_u}90 \qquad\qquad (A.12)$$

$$Q_{12_m} = Q_{12_u}0 + Q_{12_u}90$$

$$Q_{66_m} = Q_{66_u}0 + Q_{66_u}90$$

where the 0 and 90 represent the two fiber directions. The ratio K is defined to be $K = \frac{Q_{11_u}0}{Q_{22_u}90} = \frac{Q_{11_u}90}{Q_{22_u}0}$. Assuming that the Q_{12} and Q_{66} terms are equal for both directions, the unidirectional material properties are;

$$Q_{11_u}0 = \frac{K}{K+1} Q_{11_m}$$

$$Q_{22_u}0 = \frac{1}{K+1} Q_{22_m}$$

$$Q_{11_u}90 = \frac{K}{K+1} Q_{22_m} \qquad\qquad (A.13)$$

$$Q_{22_u}90 = \frac{1}{K+1} Q_{11_m}$$

$$Q_{12_u}0 = Q_{12_u}90 = \frac{Q_{12_m}}{2}$$

$$Q_{66_u}0 = Q_{66_u}90 = \frac{Q_{66_m}}{2}$$

where Q_{11_m}, Q_{22_m}, Q_{12_m} and Q_{66_m} are the overall material properties calculated in equation (A.8).

One can now assemble the stiffness matrix for any laminate, with any misalignment angle α, by sutstituting the unidirectional values given in equation (A.7) for [Q']. If the lamina is oriented at same angle Θ to the structural axes, by using the appropriate transformations, one obtains the stress-strain relationship in structural coordinates to be:

$$
\begin{bmatrix} \sigma_x \\ \sigma_y \\ \tau_{xy} \end{bmatrix}
=
\begin{bmatrix} \bar{Q}_{11} & \bar{Q}_{12} & \bar{Q}_{16} \\ \bar{Q}_{12} & \bar{Q}_{22} & \bar{Q}_{26} \\ \bar{Q}_{16} & \bar{Q}_{26} & \bar{Q}_{66} \end{bmatrix}
\begin{bmatrix} \varepsilon_x \\ \varepsilon_y \\ \gamma_{xy} \end{bmatrix}
\qquad (A.14)
$$

where $\bar{Q}$ is defined as

$$\bar{Q}_{11} = Q_{11}m^4 - 4Q_{16}m^3n + 2(Q_{12} + 2Q_{66})m^2n^2 - 4Q_{26}mn^3 + Q_{22}n^4$$

$$\bar{Q}_{12} = Q_{12}(m^4 + n^4) + 2(Q_{16} - Q_{26})m^3n + (Q_{11} + Q_{22} - 4Q_{66})m^2n^2$$

$$+ 2(Q_{26} - Q_{16})mn^3$$

$$\bar{Q}_{16} = Q_{16}m^4 + (Q_{11} - Q_{12} - 2Q_{66})m^3n + 3(Q_{26} - Q_{16})m^2n^2$$

$$+ (Q_{12} - Q_{22} + 2Q_{66})mn^3 - Q_{26}n^4$$

$$\bar{Q}_{22} = Q_{22}m^4 + 4Q_{26}m^3n + 2(Q_{12} + 2Q_{66})m^2n^2 + 4Q_{16}mn^3 + Q_{11}n^4 \quad \text{(A.15)}$$

$$\bar{Q}_{26} = Q_{26}m^4 + (Q_{12} - Q_{22} + 2Q_{66})m^3n + 3(Q_{16} - Q_{26})m^2n^2$$

$$+ (Q_{11} - Q_{12} - 2Q_{66})mn^3 - Q_{16}n^4$$

$$\bar{Q}_{66} = Q_{66}(m^4 + n^4) + 2(Q_{16} - Q_{26})m^3n + 2(Q_{26} - Q_{16})mn^3$$

$$+ (Q_{11} - 2Q_{12} + Q_{22} - 2Q_{66})m^2n^2$$

and $\qquad m = \cos \Theta$

$\qquad\qquad n = \sin \Theta$

The summation through the thickness of the laminate is then performed in the standard way to give the terms,

$$A_{ij} = \sum_{k=1}^{N} \bar{Q}_{ij} (h_k - h_{k-1})$$

$$B_{ij} = \frac{1}{2} \sum_{k=1}^{N} \bar{Q}_{ij} (h_k^2 - h_{k-1}^2) \qquad\qquad (A.16)$$

$$D_{ij} = \frac{1}{3} \sum_{k=1}^{N} \bar{Q}_{ij} (h_k^3 - h_{k-1}^3)$$

where k = ply number

h_k = position of the top surface of the ply relative to the centre
of the specimen

N = number of plies.

The terms A, B, D relate the applied loads and moments to the strains and curvatures by the equations,

$$
\begin{bmatrix} N \\ \hline M \end{bmatrix}
=
\begin{bmatrix} A & B \\ \hline B & D \end{bmatrix}
\begin{bmatrix} \varepsilon^0 \\ \hline K \end{bmatrix}
\qquad\qquad (A.17)
$$

Equation (A.17) can then be inverted to give the strains and curvatures in terms of the loads such that

63

$$
\begin{bmatrix} \varepsilon^0 \\ -- \\ K \end{bmatrix} = \begin{bmatrix} A' & | & B' \\ --|-- \\ B' & | & D' \end{bmatrix} \begin{bmatrix} N \\ -- \\ M \end{bmatrix} \qquad (A.18)
$$

Knowing the applied loads N and moments M, the in-plane strains ε^0 and curvatures K can be calculated from equation (A.18).

At this point, the stresses in the individual lamina can be calculated in order to determine the load required for failure. The equation for the stress in the k-th ply is, in the lamina fiber directions,

$$
[\sigma]_k = [T][\bar{Q}]_k[\varepsilon^0] + Z[T][\bar{Q}]_k[K] \qquad (A.19)
$$

where Z is the position of the ply from the laminate mid-plane, and [T] is the transformation matrix

$$
[T] = \begin{bmatrix} m^2 & n^2 & 2mn \\ n^2 & m^2 & -2mn \\ -mn & mn & m^2-n^2 \end{bmatrix} \qquad (A.20)
$$

where $m = \cos\Theta$

          $n = \sin\Theta$

          Θ = angle of rotation from structural axes.

The equations given above are for a standard unidirectional material, and need to be modified for the misaligned material under investigation.

64

Several approaches can be used to calculate the stress and failure loads for the weave material.

The failure equation to be used is a tensor polynomial failure criterion based on the lamina stresses. The equation is,

$$F_i \sigma_i + F_{ij} \sigma_{ij} + F_{ijk} \sigma_i \sigma_j \sigma_k + \ldots = 1 \qquad \text{(A.21)}$$

where $i,j,k = 1,2,6$

$$F_i, \ F_{ij}, \ F_{ijk} \ \ldots \text{ are the strength tensors.}$$

Initially a quadratic equation will be used for the strength analysis. Equating F_{ij} to F_{ji} and noting that all odd order terms in σ_6 are zero, equation (A.21) reduces to

$$F_1 \sigma_1 + F_2 \sigma_2 + F_{11} \sigma_1^2 + F_{22} \sigma_2^2 + F_{66} \sigma_6^2 + 2F_{12} \sigma_1 \sigma_2 = 1 \qquad \text{(A.22)}$$

These F terms can be calculated from unidirectional tension, compression and shear tests on 0° and 90° specimens and a combined σ_1-σ_2 test for the F_{12} term. The following section describes the stress and failure analysis methods which can be used.

The first method is to use equation (A.19) directly for the stresses. This will not change the stress-load ratio as the misalignment angle changes. It would then be necessary to calculate the strength parameters F_i, F_{ij} as a function of the misalignment angle. The problem with this method is that many tests are required to find the strength tensors as a function of the misalignment angle. Because of the number of tests required, this method was not used.

A second method is to alter the transformation matrix (equation A.20) so that the stresses σ_1 and σ_2 are parallel to the fibers in the misaligned material. This can be easily done and provides for the additional stress in the fiber directions due to the misalignment. The problem with this method is that the effect of the shear strain is not accounted for, since the shear stress is equal to zero. For this reason an alternate solution was needed.

The method which we decided to use was to modify the $\bar{Q}$ matrix to account for the different strain states. What is done is to apply the strains and curvatures calculated using the misaligned material properties, to an aligned material. In this way the shear strain is equated to an equivalent shear stress as well as altering the stresses in the fiber directions. This stress state is then put into the failure equation (A.22) using the strength terms from the aligned material tests. In effect what is being done here is to consider the problem to be a strain failure equation, since the results obtained are the same as one would get if you converted the F terms into strain space from stress space, then solving the problem using the strains resulting from the misaligned material. As can be seen in Figures 12 and 13, this analysis provides reasonably good agreement with the experimental strength and modulus data. The ratio of fiber to transverse modulus in the unidirectional material K is varied to examine it's effect. As can be seen in Figures 12 and 13, the effect of varying K is minimal and the average value of K=15 will be used for further analysis.

The other type of analysis which can be used is to consider the material fibers to have remained perpendicular to each other, and the entire material rotated about the structural axes. The standard analysis for an off-axis specimen is used and the results are presented in Figures 12 and 13 for comparison with the other theories. As can be seen, this method predicts the modulus much the same as the other method, but it vastly

overpredicts the strength. As a result, this analysis should not be used for material strength predictions to account for misaligned fibers.

In summary, the methodology used for this analysis is given below.

1) Calculate the material stiffness $[Q_m]$ for a perfectly aligned material;

2) Divide the material into two parts, $[Q']$ for the straight (warp direction fibers and $[Q'']$ for the misaligned (fill direction) fibers;

3) Assume a ratio of unidirectional properties for the two directions
$$K = \frac{Q_{11_u 0}}{Q_{22_u 90}} = \frac{Q_{11_u 90}}{Q_{22_u 0}} ;$$

4) Calculate $[Q']$ and $[Q'']$ in terms of $[Q_m]$, K and the misalignment angle α;

5) Assemble the stiffness matrix $[Q] = [Q'] + [Q'']$ which represents the stiffness of a single ply of misaligned material in material coordinates;

6) Rotate $[Q]$ into structural axes giving $[\bar{Q}]$ and sum over all plies to give $[A]$, $[B]$ and $[D]$, the structural stiffness matrices;

7) Invert the structural stiffness matrix to give the ratio of strains and curvatures to the applied loads and moments;

8) Knowing the applied loads, calculate the specimen strains and curvatures, then calculate the stresses resulting from applying these strains to an aligned ply;

9) Using these stresses and a quadratic tensor polynomial failure equation, calculate the loads required for failure as a function of the misalignment angle.

1. Report No. NASA CR-172465	2. Government Accession No.	3. Recipient's Catalog No.
4. Title and Subtitle Development of Failure Criterion for Kevlar/Epoxy Fabric Laminates		5. Report Date September 1984
		6. Performing Organization Code
7. Author(s) R. C. Tennyson and W. G. Elliott		8. Performing Organization Report No.
		10. Work Unit No.
9. Performing Organization Name and Address University of Toronto Institute for Aerospace Studies Toronto, Ontario, Canada		11. Contract or Grant No. NSG-7409
		13. Type of Report and Period Covered Contractor Report 8/82 - 8/83
12. Sponsoring Agency Name and Address National Aeronautics and Space Administration Washington, DC 20546		14. Sponsoring Agency Code 505-42-23-03
15. Supplementary Notes Langley Technical Monitor: Donald J. Baker Interim Report		

16. Abstract

This report describes a continued effort on the development and application of the tensor polynomial failure criterion for composite laminate analysis. In particular, emphasis in this report is given to the fabrication and testing of Kevlar-49 fabric (Style 285)/Narmco 5208 Epoxy. The quadratic-failure criterion with $F_{12}=0$ provides accurate estimates of failure stresses for the Kevlar/Epoxy investigated.

The cubic failure criterion has been re-cast into an operationally easier form, providing the engineer with design curves that can be applied to laminates fabricated from unidirectional prepregs. In the form presented no interaction strength tests are required, although recourse to the quadratic model and the principal strength parameters is necessary. However, insufficient test data exists at present to generalize this approach for all unidirectional prepregs and its use must be restricted to the generic materials investigated to-date.

17. Key Words (Suggested by Author(s)) Composite Structures Failure Analysis Laminates Modulus of Elasticity Tsi-Wu Criterion	18. Distribution Statement Unclassified - Unlimited Subject Category - 24		
19. Security Classif. (of this report) Unclassified	20. Security Classif. (of this page) Unclassified	21. No. of Pages 68	22. Price A04